KEIT-HD 70-1018

PAPER NO.

1735

EFFECTS OF ELEVATED PRESSURE AND TEMPERATURE ON NOTCHED TENSILE SPECIMENS

by

H. D. Keith and R. L. Davis
University of Missouri

Presented at

1970 SESA FALL MEETING

Boston, Mass.

October 18-22

The opinions expressed in this paper are those of the individual authors and must not be considered as necessarily representing the ideas of the Society.

MAR 12 1971

SOCIETY FOR
EXPERIMENTAL STRESS ANALYSIS
21 BRIDGE SQUARE WESTPORT, CONNECTICUT

EFFECTS OF ELEVATED PRESSURE AND TEMPERATURE ON NOTCHED TENSILE SPECIMENS

H. D. Keith

R. L. Davis

ABSTRACT

The effect of temperature and stress state on the nil ductility transition (NDT) and fracture strength of A-204, A-387, and A-515 plate steel has been investigated. Testing of notched and standard cylindrical tensile specimens at pressure and temperature extremes of 84,000 psi and 600^{o}F, respectively, indicates that the stress state is just as important as temperature in defining the NDT point and the fracture strength. A finite element program was used to evaluate the stress state occurring in the notched specimens.

INTRODUCTION

Within the past five years a revolutionary new method has evolved for performing thermoplastic analyses of complex structures. The method, which is referred to as the 'finite element' technique, is completely general with respect to geometry and material properties, and can treat arbitrary thermal and mechanical loads. The limiting factor associated with the 'finite element' technique is the lack of suitable information on material behavior under triaxial stress conditions, temperature, high loading rates, et cetera. Complete material behavior data is required not only for input to the analysis program, but for interpreting the results. Thus, even if an analysis program, such as the finite element method, does provide an accurate determination of the stress and strain state at all points within a structure, the analysis is not complete until the designer can interpret how the material will respond (i.e., yield, fracture, et cetera) under these particular conditions.

The authors of this paper have been analyzing high-pressure heat exchangers, pressure vessels, skirted process vessels, et cetera, with finite element programs. In each case the analysis indicated that critical positions in the structure were exposed to simultaneous conditions of triaxial tensile stress states and elevated temperature. There are numerous papers[1,2,3,4,5]* that provide evidence that a one-dimensional theory of failure

---

*Superscript numbers correspond to reference numbers.

is not suitable for predicting the effects of simultaneous hydrostatic stress states (tensile or compressive) and elevated temperatures. Although Thielsch[6], Lubahn[7], Biggs[8], Spath[9], Goldhoff[10], and others have shown definite trends for specific conditions and materials, it does not appear that any general quantitative conclusions on material response can be made at this time. For this reason, the authors elected to test a number of typical vessel materials (A-204, A-387, and A-515 plate steel) under known triaxial stress states and elevated temperatures, and present the results in a form that will assist in the evaluation of the output from an analysis program.

SPECIMEN DESCRIPTION AND ANALYSIS

The notched cylindrical tensile specimen shown in Fig. 1 has been selected as the means for generating triaxial tensile stresses. The symbology defined in Table I describes the location and orientation of each specimen relative to the original plate.

TABLE I

Data Symbol	Location	Orientation
△	Outside	Direction of Roll
□	Outside	Long Transverse Direction
○	Inside	Direction of Roll
⬡	Inside	Long Transverse Direction

Specimen Orientation and Location Relative to Original Plate

By testing both notched and unnotched tensile specimens in controlled high pressure and high temperature environments, the stress state can be varied from triaxial tension to triaxial compression, and the resulting material response can be recorded. Biggs[8] has summarized the results of McAdam, Lubahn, Kuntze, and others regarding the use of notched cylindrical specimens for determining the effects of triaxial stresses on flow and fracture. In each of the cases cited, the lack of a suitable method for evaluating the stress state in the vicinity of the notch root, especially after yielding had occurred, appeared to be the most limiting factor.

Marcal and King[11] used the finite element method to establish the spread of the elastic-plastic interface in a 90°-notched (zero notch tip radius) perfectly plastic cylindrical tensile specimen. Following the approach of Marcal, the authors of this paper have utilized a finite element analysis to determine the stress state in a 60°-notched specimen having a 0.0085-inch notch tip radius. The finite element grid used in the analysis contained 445 elements with an element size of 0.0015-inch by 0.0015-inch in the region of the notch root. The propagation of the plastic zone is shown in Fig. 2 for A-387 steel, and the effective stress (defined in equation 1) distribution corresponding to the ultimate load (ambient environment) is presented in Fig. 3. The mean stress (hydrostatic component of stress) distribution is given in Fig. 4. The stress-strain curves (Fig. 5) which are used in the finite element program are obtained by performing uniaxial tension tests with unnotched specimens in controlled hydrostatic pressure environments.

Goldhoff[10] has provided visual evidence that crack initiation usually occurs at subsurface locations in notched cylindrical tensile specimens. The exception to this rule occurs when a suitably oriented grain boundary intersects the notch root. According to Fig. 4, this would suggest that crack initiation is governed more by the magnitude of the mean stress (hydrostatic component of the stress state) than by the effective stress. The data presented later in this paper suggests that it is a combination of both the mean stress and effective stress that governs fracture initiation.

The effective stress (σ_e) is defined as

$$\sigma_e = \frac{1}{\sqrt{2}} \left[(\sigma_r - \sigma_\theta)^2 + (\sigma_\theta - \sigma_z)^2 + (\sigma_z - \sigma_r)^2 + 6\tau_{rz}^2 \right]^{\frac{1}{2}} \quad (1)$$

where σ_r, σ_θ, σ_z are the radial, circumferential, and axial normal stresses, respectively, and τ_{rz} is the only non-vanishing tensorial shear stress. Based on the effective stress or octahedral shear stress parameter, the finite element analysis provides an elastic stress concentration factor of 3.56. The equations developed by Neuber[12] predict a stress concentration factor, based on the maximum shear stress, of 3.51.

EXPERIMENTAL PROCEDURE AND RESULTS

The experimental program involved the testing of notched and unnotched tensile specimens of A-204, A-387, and A-515 steel in hydrostatic pressure and elevated temperature environments ranging up to 84,000 psi and 600°F, respectively. The triaxial tensile stresses that are present in the notched specimens are calculated by the finite element method, thus providing information regarding the stress states that occur during ambient loading conditions. By testing notched specimens in increasing pressure environments, the effects of superimposing triaxial compressive stresses can be determined. Likewise, if the notched specimens are tested in elevated temperature environments, the effects of temperature and triaxiality of the stresses can be assessed. Uniaxial testing of unnotched specimens in similar pressure or temperature environments provides accepted material response data, at least up to the ultimate point, and, as will be seen later, is quite useful in the construction of an effective stress-mean stress diagram.

The testing facilities are shown schematically in Fig. 6. Once the desired pressure-temperature conditions are obtained within the vessel, the compression machine is started and the ram is forced further into the vessel. The downward force of the ram is converted into a tensile load on the specimen by the action of the yoke assembly shown in Fig. 7. A bleed-valve is used to maintain a constant environmental pressure

during the loading process. The specimen load-deflection is monitored continuously on a chart recorder during each test.

The fracture surfaces of both notched and unnotched A-387 steel specimens that were ruptured under increasing pressure and temperature environments are shown in Figs. 8, 9, 10, and 11, respectively. These sketches, which were drawn at a magnification of 18X, were used to define the diameter and the radius of curvature of the contour of the neck. It is apparent from Figs. 8 through 11 that, for the ranges of pressure and temperature investigated, pressure contributes more to the increase in reduction in area than does the temperature.

The effects of increasing environmental pressure and temperature on the yield strength, true strain at fracture, elongation, ultimate load, and ultimate stress of both notched and unnotched tensile specimens of A-387 steel are shown in Figs. 12 through 16. Similar data for A-204 and A-515 steel is presented in Figs. 17 through 21 and Figs. 22 through 26, respectively. The isotropy and homogeneity of each plate material (all materials where supplied in the form of 2-inch thick plates) was investigated by taking specimens from the interior and outside surface, and in the direction of roll and in the long transverse direction. The symbolism describing the specimen orientation and location relative to the plate has been given in Table I. While certain deviations have occurred, there appears to be ample evidence that the plates tested are essentially isotropic and homogeneous.

The effect of temperature on the yield and ultimate stress, as shown in Figs. 12, 13, 17, 18, 22, 23, is similar to that recorded by Clough in Reference 3. The true strain at fracture (Figs. 14, 19, and 24) decreases with an increase in temperature for A-387 steel, but reaches a minimum at approximately 400^{o}F and begins to increase with increasing temperature for A-204 and A-515 steel.

As shown in Figs. 14, 19, 24, the true strain at fracture increases with an increase in the environmental pressure. This phenomenon has also been recognized by Hu[2] and Beresnev[13] in their studies on brass. There appears to be only a slight increase in yield strength with increasing pressure (up to 50,000 psi) which is consistent with the findings of Bridgman[14].

Figs. 15, 16, 20, 21, 25, 26 indicate that the effects of pressure and temperature on the strength and ductility of notched specimens is similar to that found for standard tension specimens. The axial deformation recorded in Figs. 16, 21, and 26 is the total deflection of the specimen.

The data and discussion presented in Reference 4 supports the idea of using an effective stress (σ_e)-mean stress (σ_m) diagram for displaying fracture data. The stress state occurring in the neck of an unnotched tensile specimen is evaluated by using the Parker[16] correction factor which gives a slightly higher stress state at the specimen axis than the corresponding Bridgman[14] factor. Since fracture first occurs at the center of the neck region in a standard cylindrical tension specimen, the effective stress-mean stress at this point is used in the

construction of Fig. 27. In the notched specimen the point of fracture initiation is not always at the same subsurface location. Thus, the effective stress-mean stress values (as determined by finite element analysis with the specimen subjected to the experimentally obtained fracture load) at each element in the neighborhood of the notch root is plotted. Since one or more of these points represents the conditions required for fracture initiation, the fracture envelope will pass through the points having the extreme values of effective stress and mean stress. Data taken from both notched and unnotched specimens tested in increasing pressure environments can be evaluated in a similar manner and plotted on the same diagram to give the results shown in Fig. 27.

Thielsch[6] has presented a diagram (reproduced in Fig. 28) of total energy absorbed versus testing temperature to illustrate the influence of notch severity on the nil ductility transition (NDT) temperature. Since the effect of a notch is to introduce triaxial tensile stresses, it appears logical that a diagram of energy absorbed-temperature-mean stress would be quite useful for illustrating the role of pressure (tensile or compressive) on the NDT temperature. Such a diagram has been constructed in Fig. 29.

CONCLUSIONS

The finite element method of analysis has provided a means for evaluating the stress state at fracture in specimens having complex geometries. As a particular example, the stress state that occurs in heated and pressurized notched cylindrical tensile specimens has been investigated and used as a means for describing the effects of temperature and triaxiality of the stresses on the ductility and fracture of A-204, A-387, and A-515 plate steel. Numerous graphs have been used to illustrate the experimental data acquired in various pressure and temperature environments. A diagram of effective stress-mean stress appears to be quite suitable for showing the effect of stress state on fracture strength. Likewise, there appears to be some merit in using an energy absorbed-temperature-mean stress diagram as a model for illustrating the influence of temperature and stress state on the material ductility.

ACKNOWLEDGEMENTS

The authors are deeply grateful to Mr. Ralph Ecoff of the Nooter Corporation (St. Louis) for the initiation of this project, and to the Nooter Corporation for its sponsorship. Thanks are also extended to Mr. Paul Smith and Mr. Patrick Davidson for their support in the experimental program, and to Mr. Kurt Hambacker for his assistance in applying the finite element and plotting programs.

REFERENCES

1. Stassi-D'Asis, F. - "A Limiting Condition of Yielding and Its Experimental Confirmations". Industria Grafica Nazionale. Palermo, Italy.

2. Hu, L. W. - "Determination of the Plastic Stress Strain Relations in Tension for Nittany No. 2 Brass Under Hydrostatic Pressure". 1958. Proc. 3rd U.S. National Congress of Applied Mechanics.

3. Clough, W. R., et al. - "The Rosette, Star, Tensile Fracture". Journal of Basic Engineering, Trans. of the ASME. March, 1968.

4. Davis, R. L. - "A Macroscopic Model Depicting Material Response Under Variable Pressures". Physical Properties of Solids Under Pressure. Grenoble. 1969.

5. Coffin, L. F., Jr. - "The Flow and Fracture of a Brittle Material". Journal of Applied Mechanics. 1949.

6. Thielsch, H. - Defects and Failures in Pressure Vessels and Piping. Reinhold. New York. 1965.

7. Lubahn, J. D. - "Optimum Carbon Content for Tempered Martensitic Steels". Journal of Basic Engineering, Trans. of ASME. March, 1968.

8. Biggs, W. D. - The Brittle Fracture of Steel. MacDonald and Evans LTD. London. 1960.

9. Spath, W. - Impact Testing of Materials. Gordon and Breach. New York. 1961.

10. Goldhoff, R. M., and Brothers, A. J. - "The Influence of Notches on Mechanical Behavior at Elevated Temperatures: Some Metallographic Observations". Journal of Basic Engineering, Trans. of ASME. March, 1968.

11. Marcal, P. V., and King, I. P. - "Elastic-Plastic Analysis of Two-Dimensional Stress Systems by the Finite Element Method". International Journal of Mech. Science. Pergamon Press. Vol. 9, pp. 143-155. 1967.

12. Neuber, H. - Theory of Notch Stresses. Springer Publishers. Berlin. pp. 222-225. 1958.

13. Beresnev, B. I., et al. - Some Problems of Large Plastic Deformation of Metals at High Pressures. Macmillan Co., New York, 1963.

14. Bridgman, R. W. - Studies in Large Plastic Flow and Fracture. Harvard University Press. 1964.

15. ASME Boiler and Pressure Vessel Code. Division 2, Section VIII. 1968. p. 40-41.

16. Parker, E. R., et al. - "A Study of the Tension Test". Proc. ASTM, 46. pp. 1159. 1949.

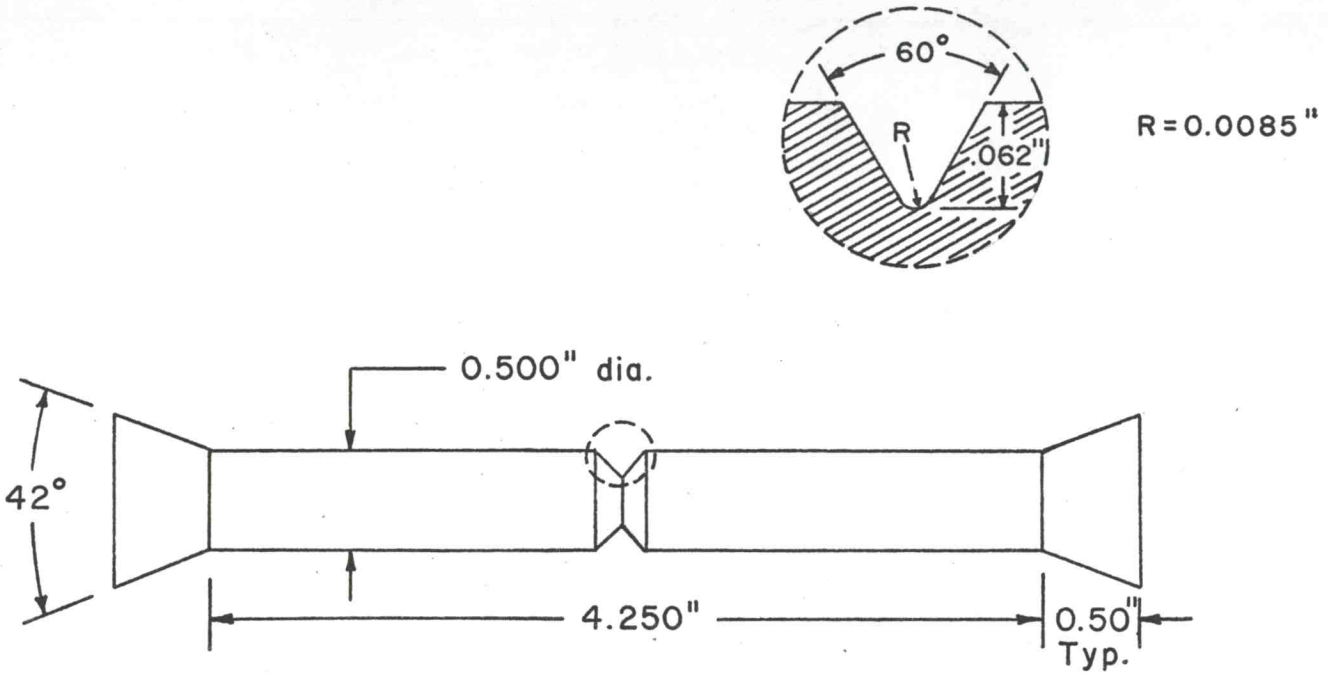


FIG. 1. NOTCHED SPECIMEN GEOMETRY

THE NUMBERS PLACED NEXT TO THE ELASTIC - PLASTIC BOUNDARIES GIVE THE CORRESPONDING APPLIED LOADS IN UNITS OF THE FIRST YIELD LOAD.

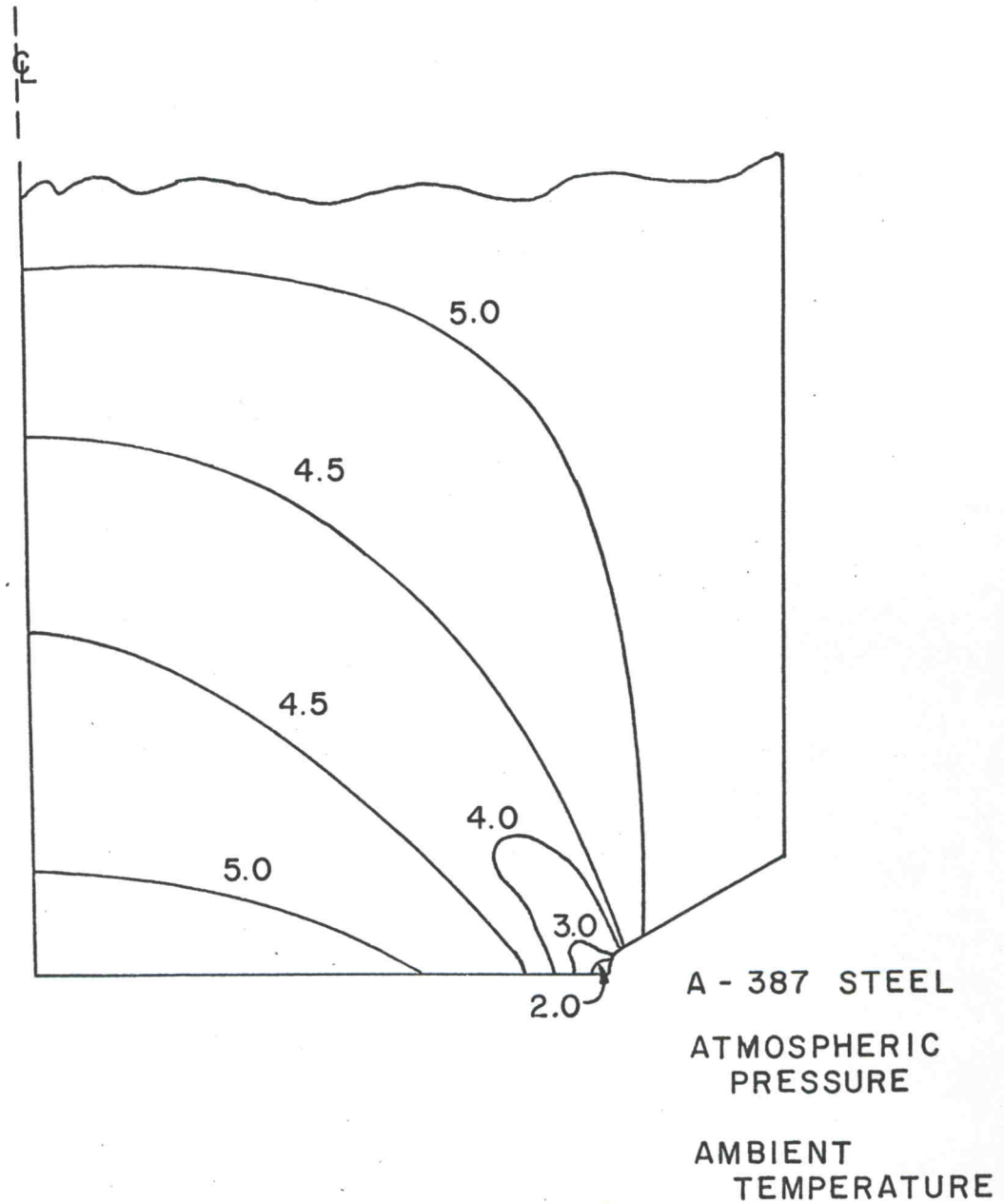


FIG. 2 PROPAGATION OF PLASTIC ZONE FOR NOTCHED SPECIMEN

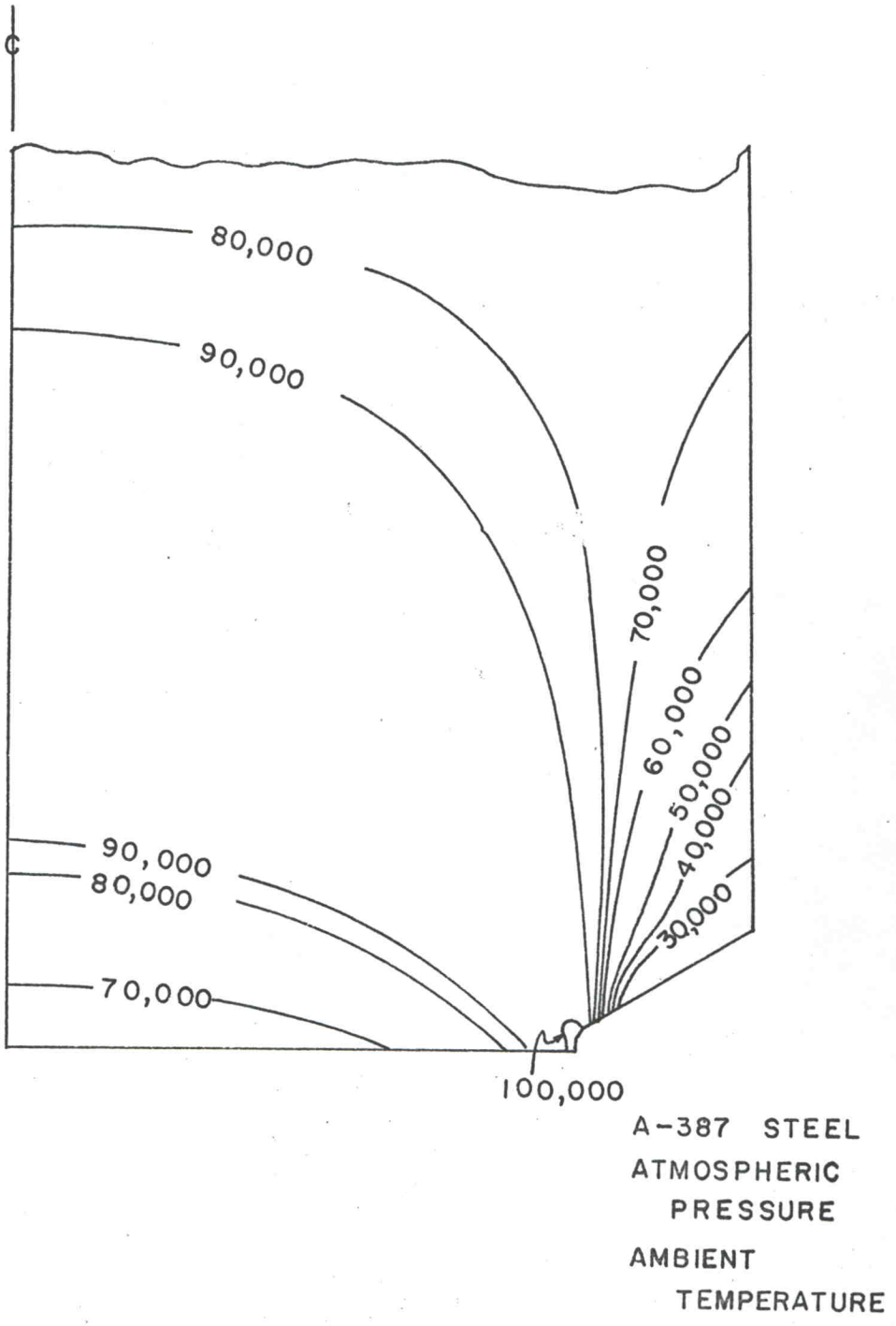


FIG. 3. EFFECTIVE STRESS DISTRIBUTION IN SPECIMEN AT ULTIMATE LOAD

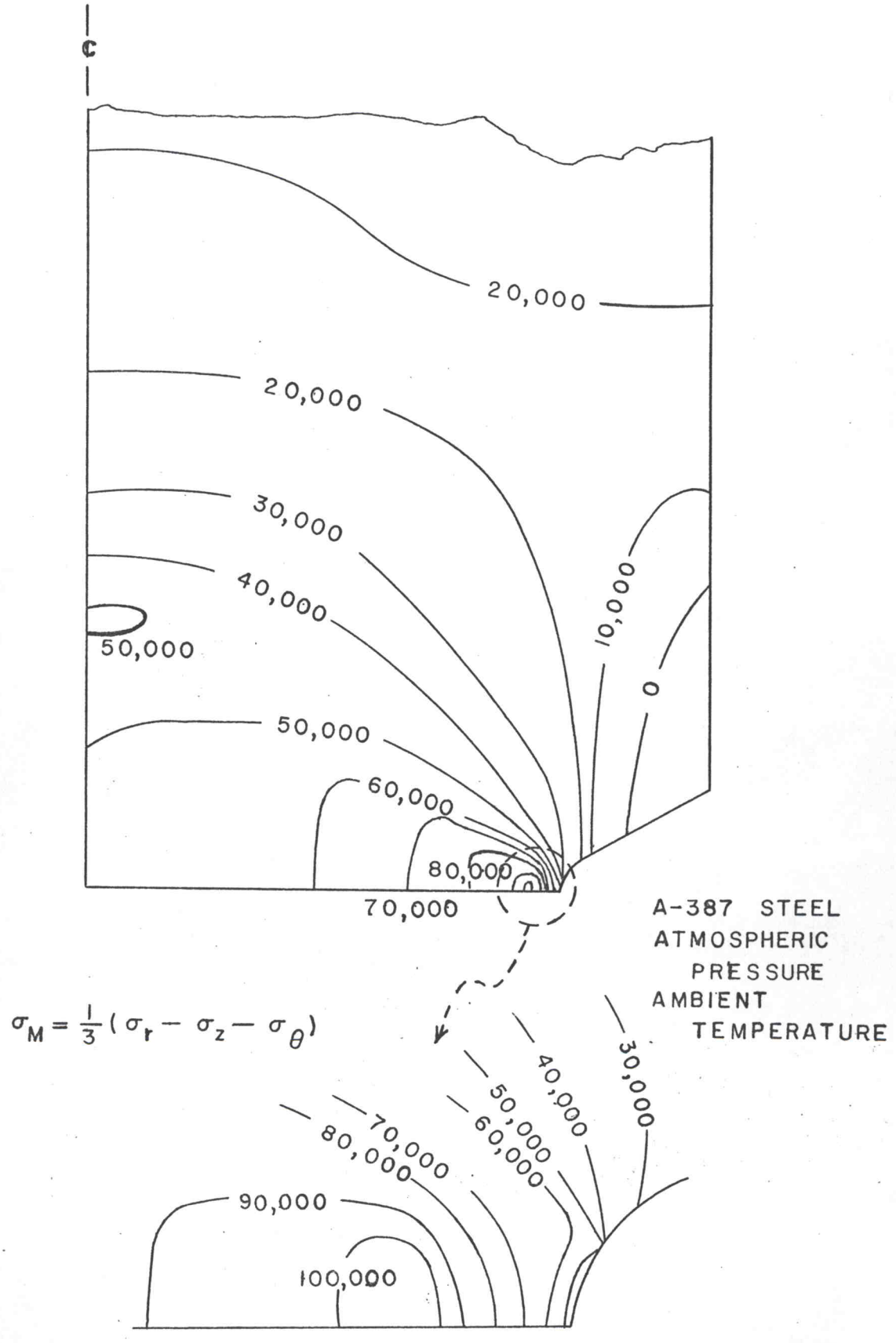


FIG. 4. MEAN STRESS DISTRIBUTION IN NOTCHED SPECIMEN AT ULTIMATE LOAD

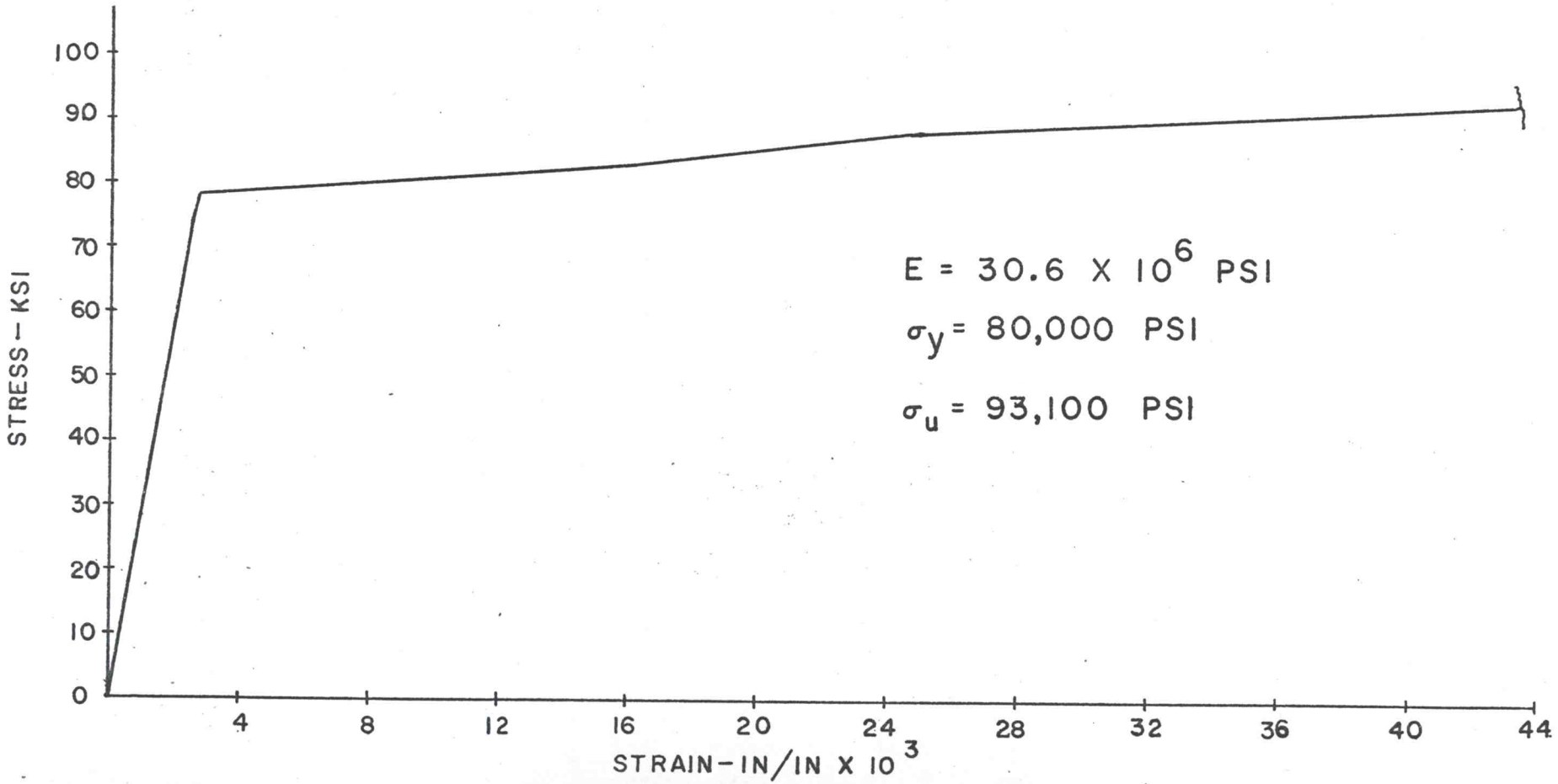


FIG. 5. UNIAXIAL STRESS STRAIN RELATION AT AMBIENT CONDITIONS FOR A-387 STEEL

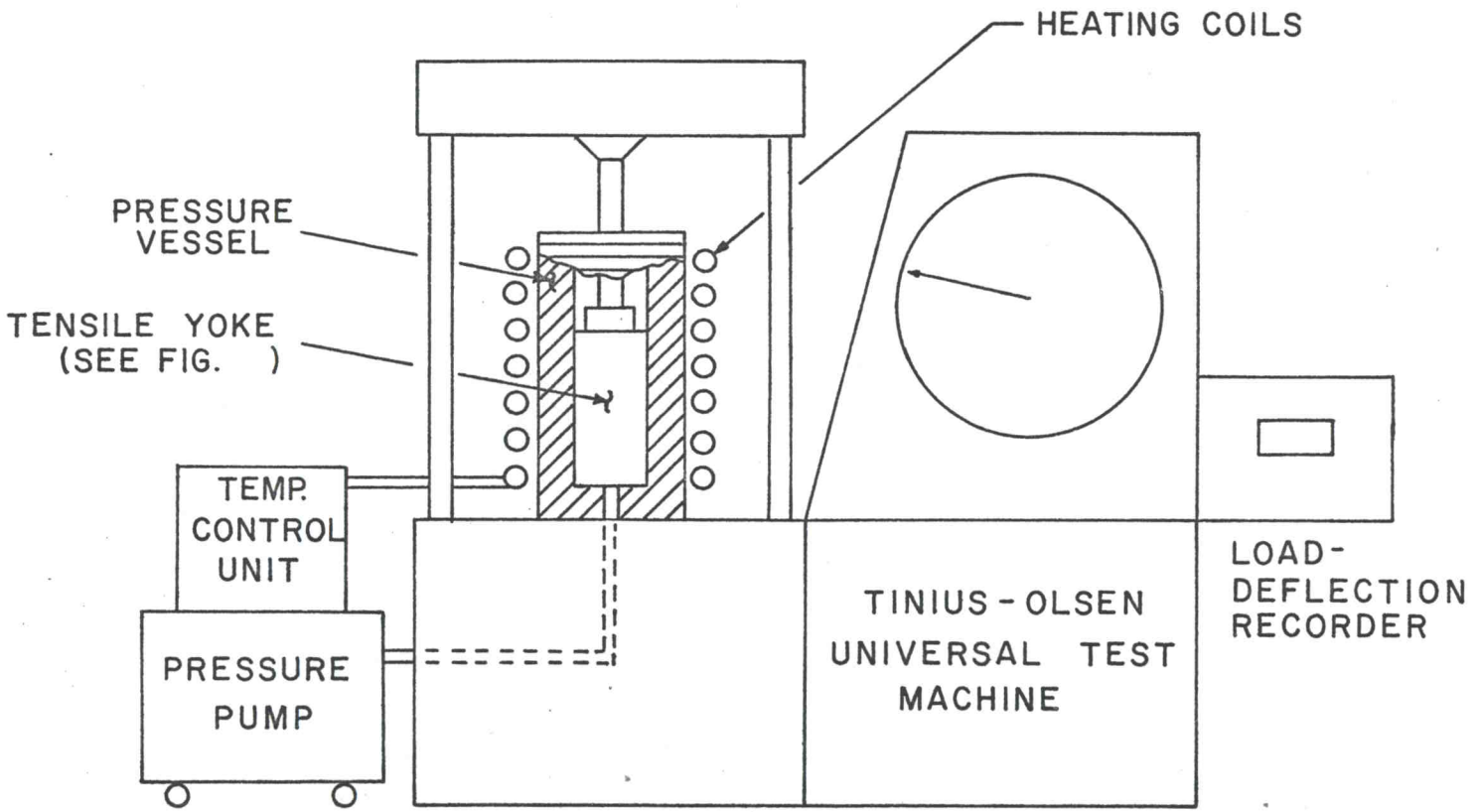


FIG. 6. TEST FACILITY

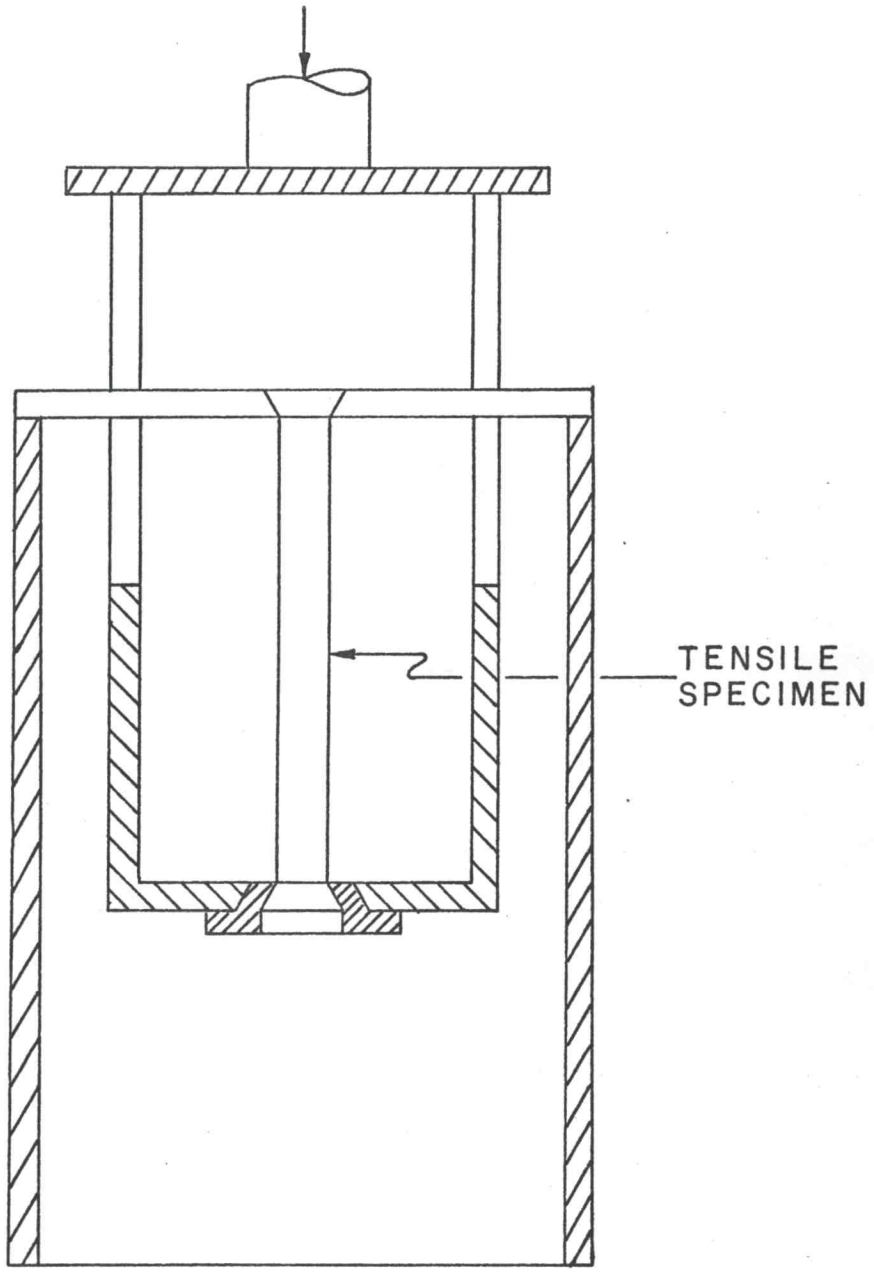


FIG. 7. YOKE ASSEMBLY FOR TENSILE TESTING

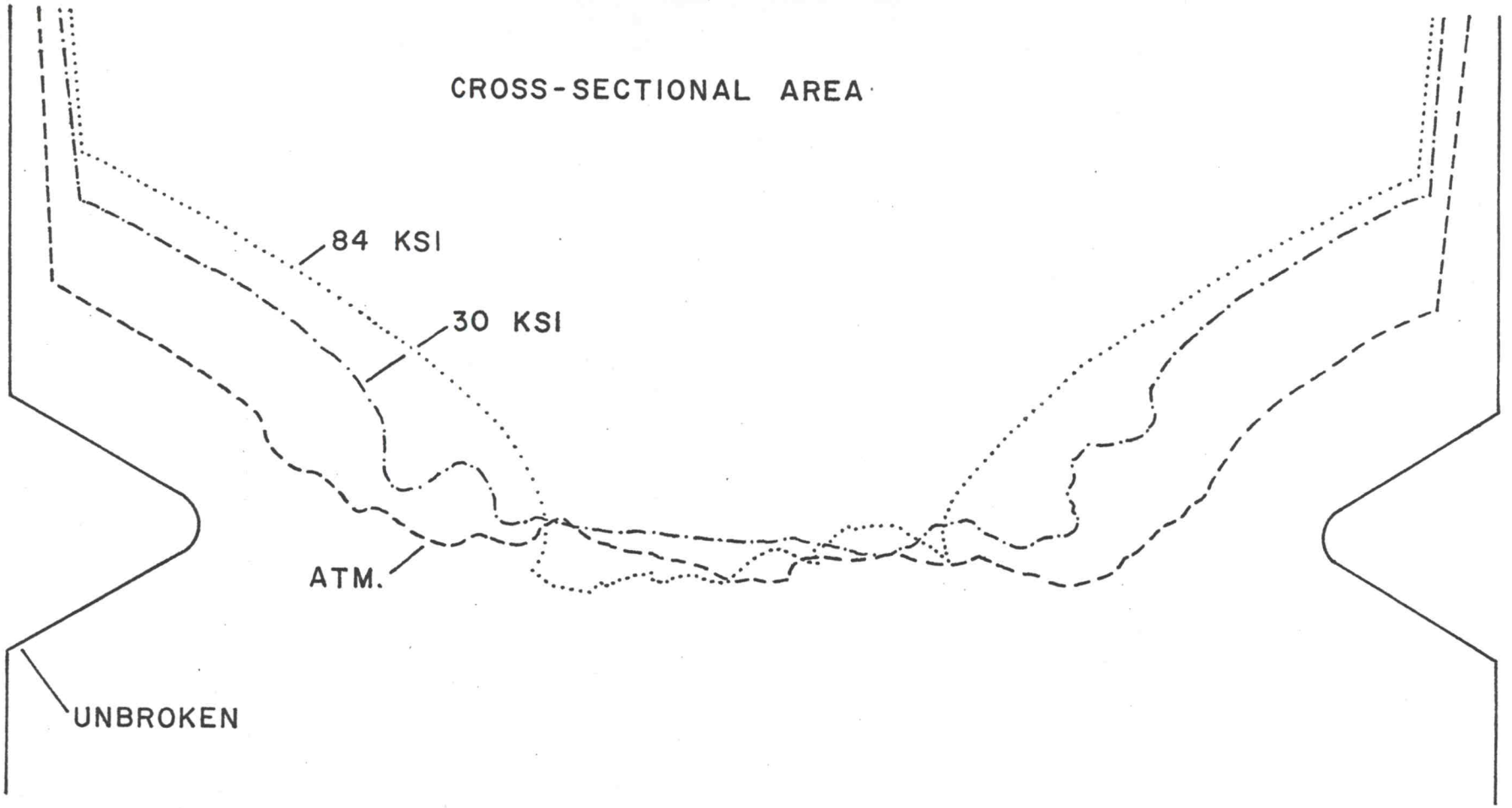


FIG. 8. EFFECTS OF ENVIRONMENTAL PRESSURE ON THE FRACTURE OF NOTCHED TENSILE SPECIMENS

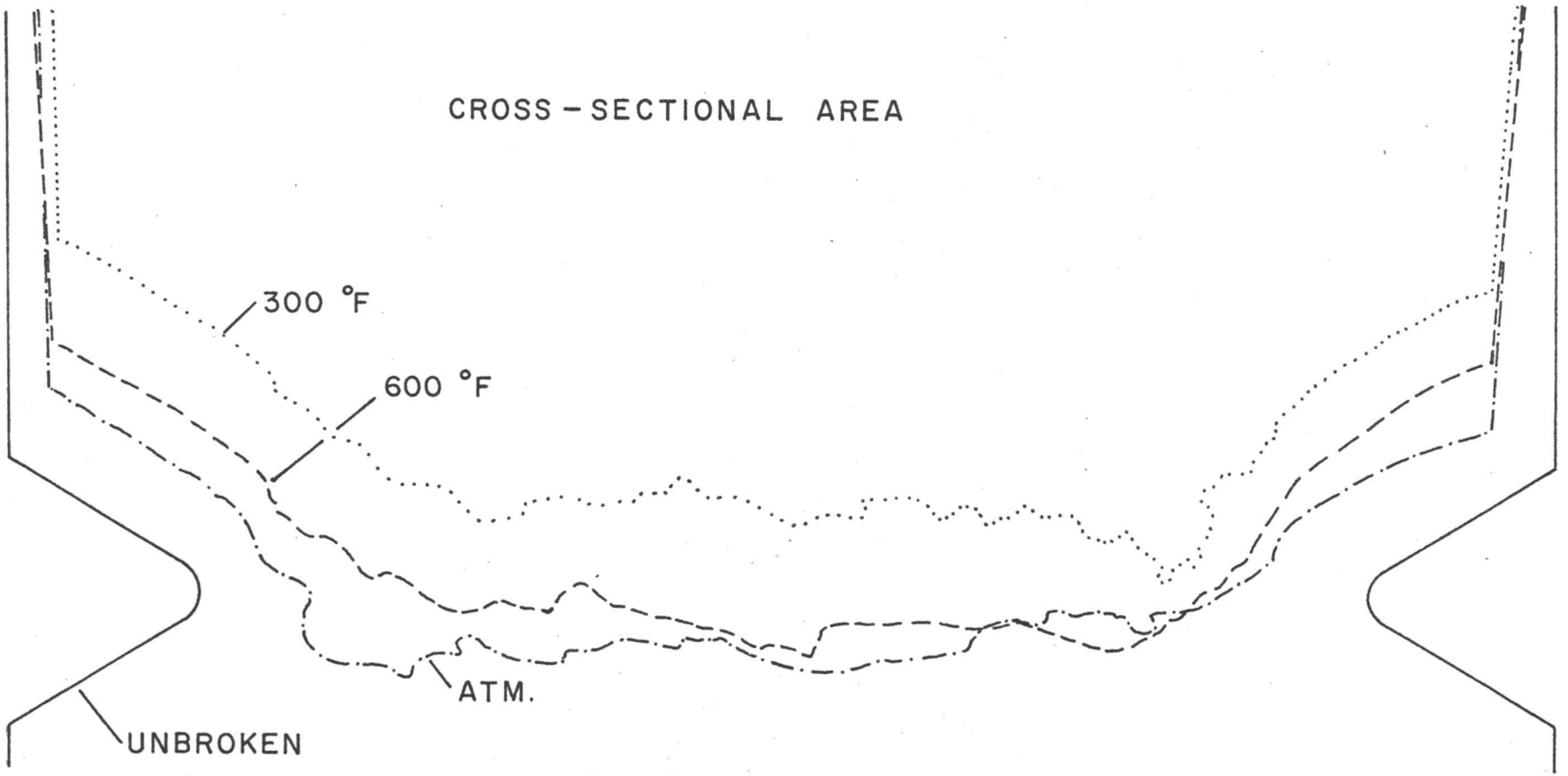


FIG. 9. EFFECTS OF TEMPERATURE ON THE FRACTURE OF NOTCHED TENSILE SPECIMENS

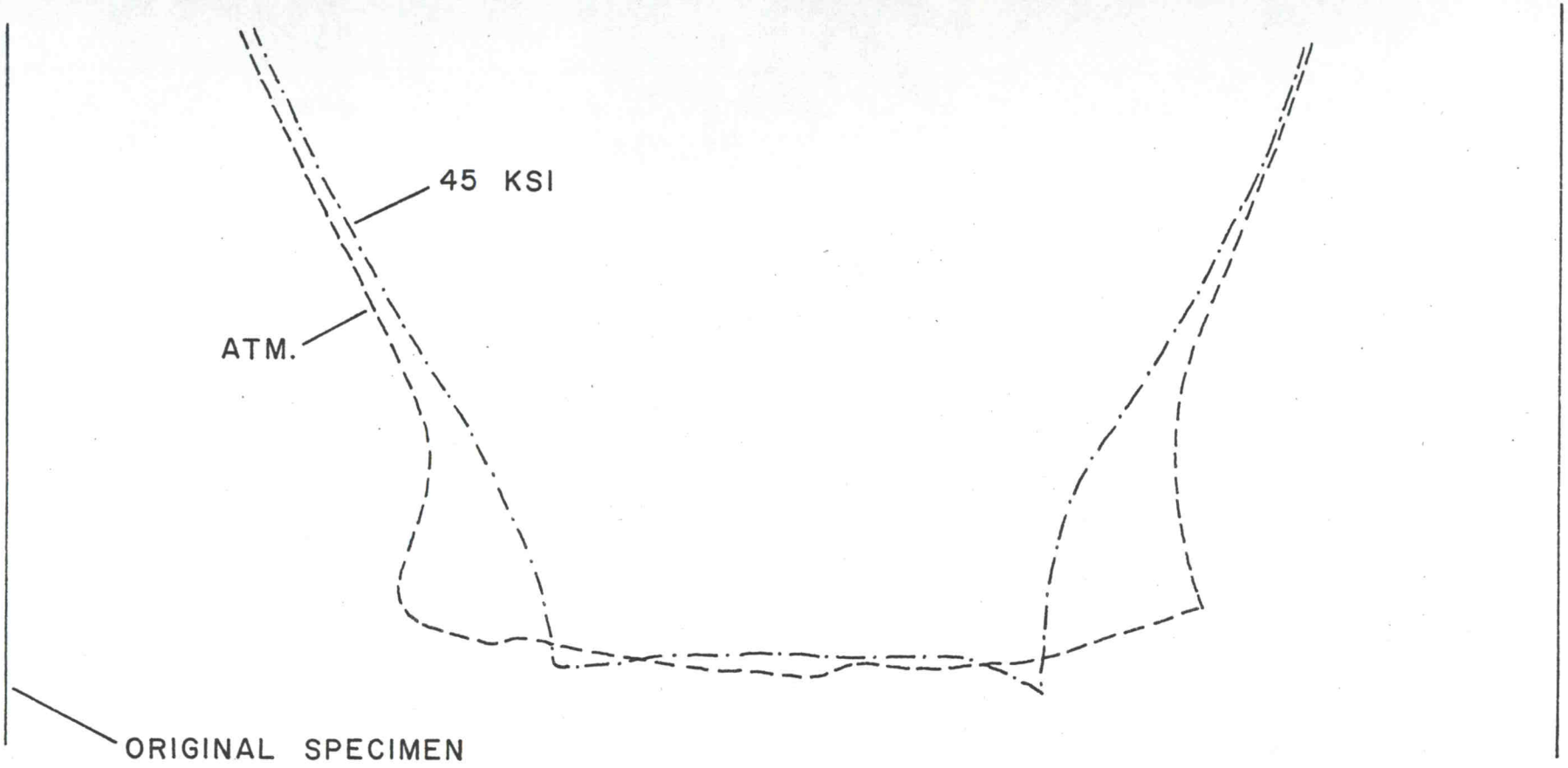


FIG. 10. EFFECTS OF ENVIRONMENTAL PRESSURE ON THE FRACTURE OF STRAIGHT TENSILE SPECIMENS

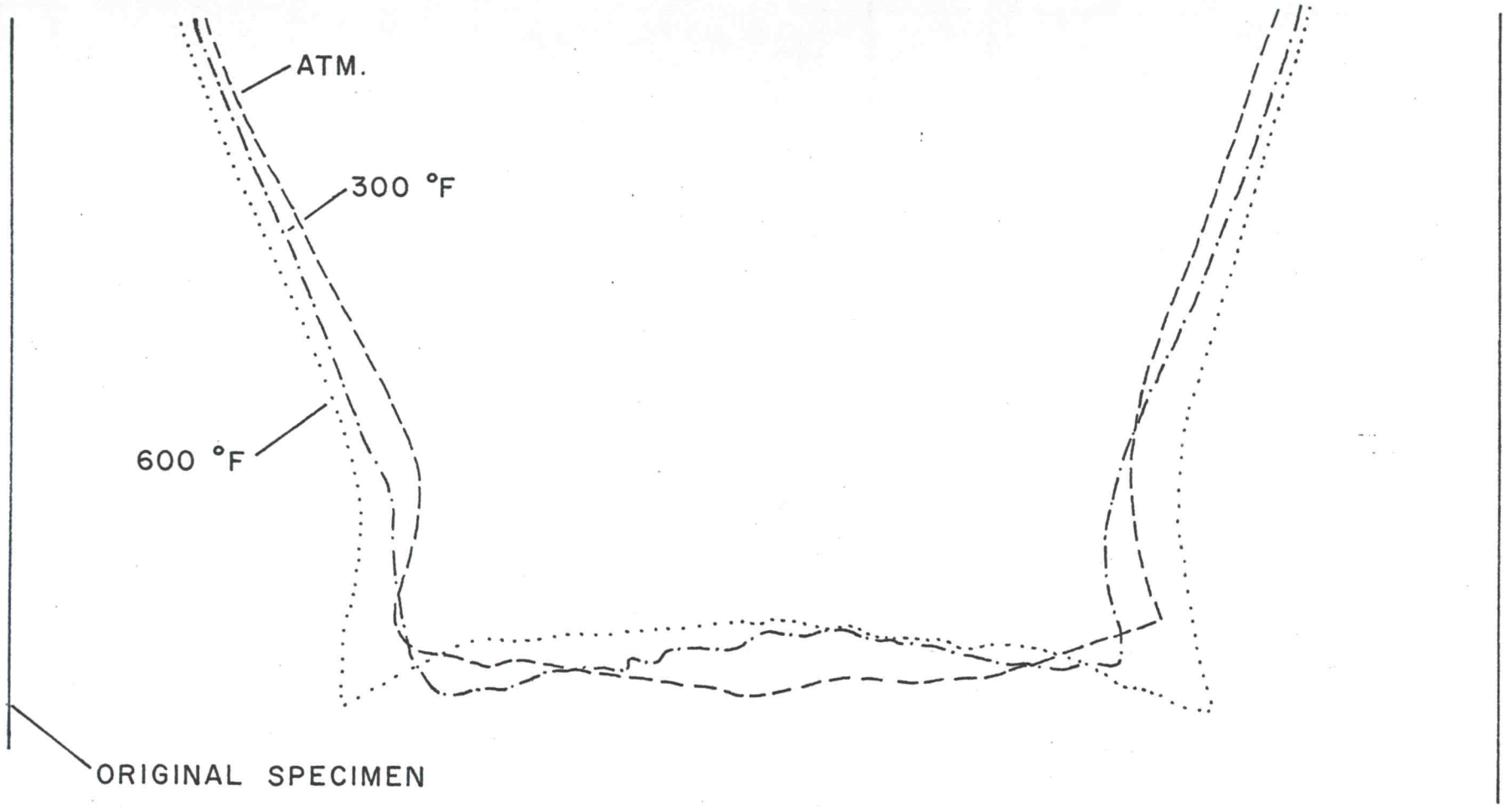


FIG. 11. EFFECTS OF TEMPERATURE ON THE FRACTURE OF STRAIGHT TENSILE SPECIMENS

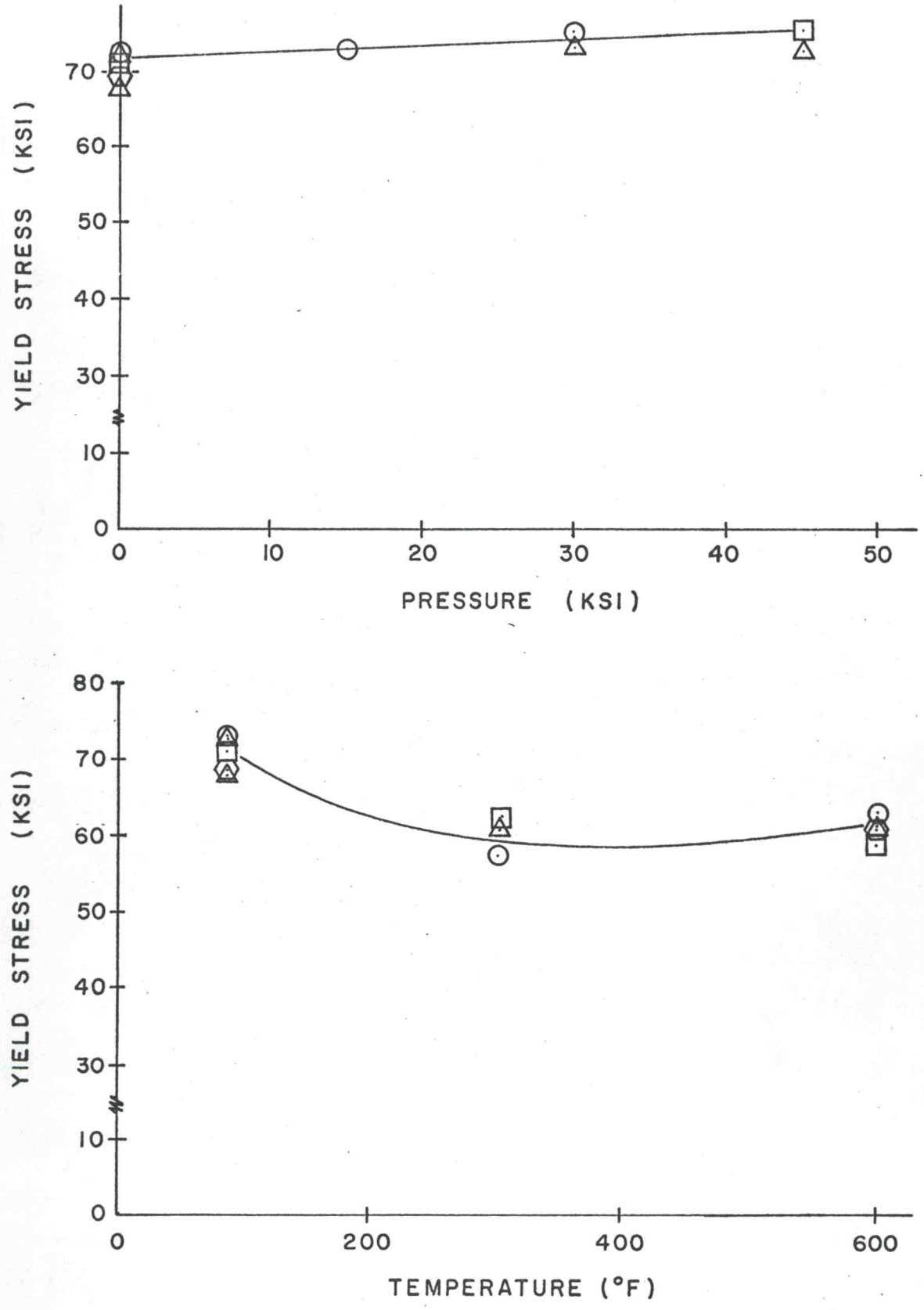


FIG. 12. EFFECTS OF ENVIRONMENTAL PRESSURE AND TEMPERATURE ON THE YIELD STRENGTH OF A-387 STEEL

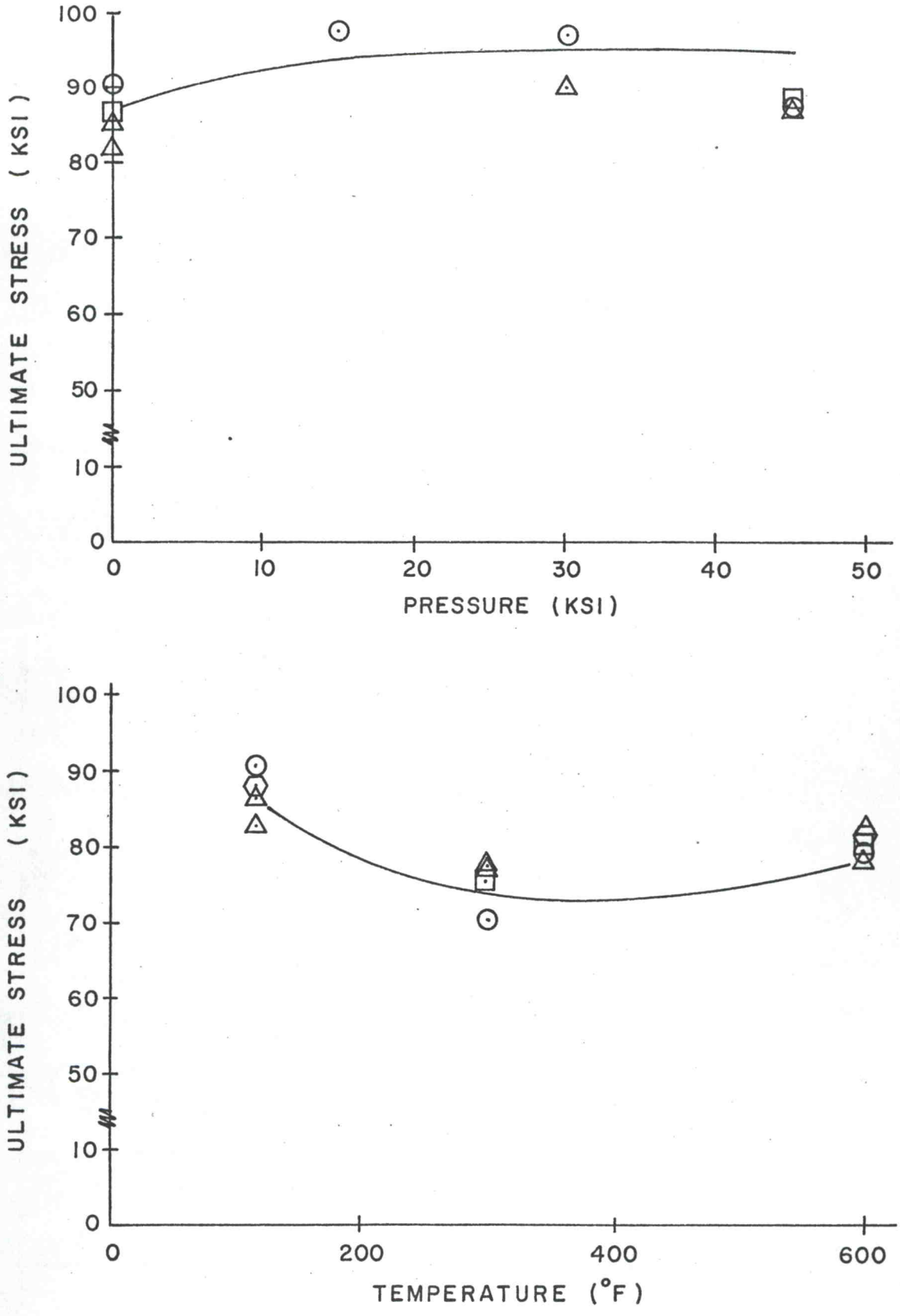


FIG. 13. EFFECTS OF ENVIRONMENTAL PRESSURE AND TEMPERATURE ON THE ULTIMATE STRENGTH OF A-387 STEEL

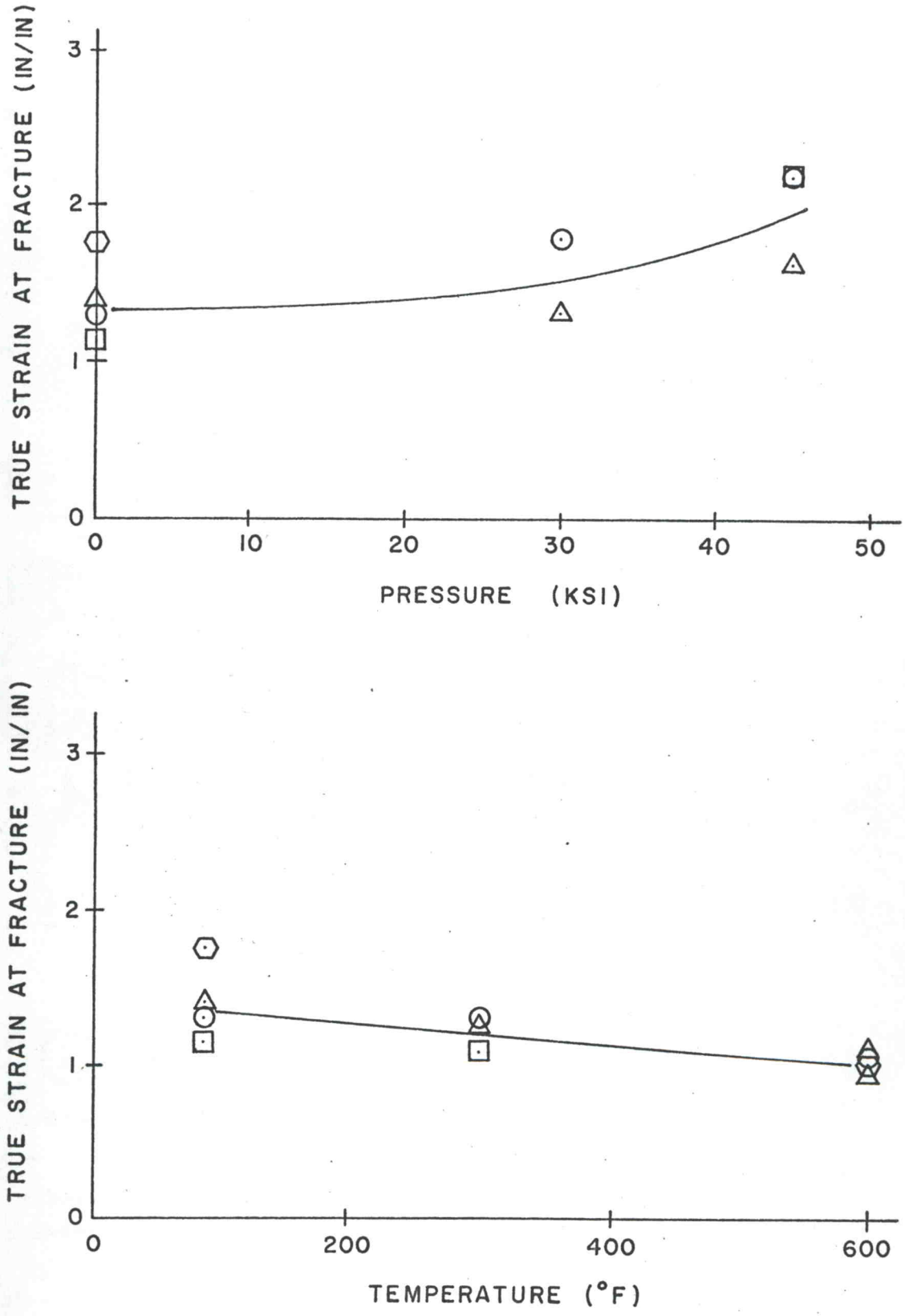


FIG. 14. EFFECTS OF ENVIRONMENTAL PRESSURE AND TEMPERATURE ON THE STRAIN AT FRACTURE OF A-387 STEEL

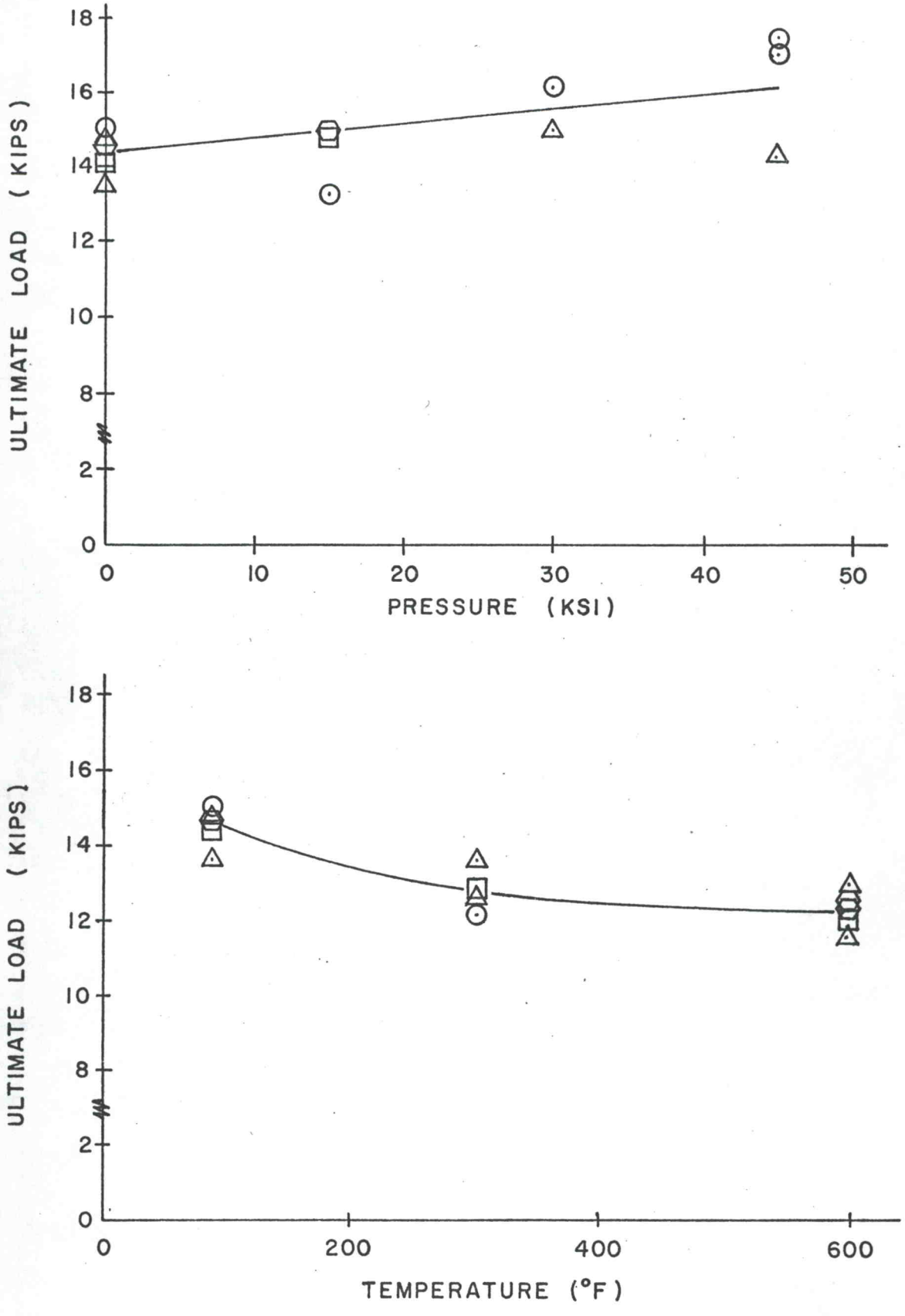


FIG. 15. EFFECTS OF ENVIRONMENTAL PRESSURE AND TEMPERATURE ON THE ULTIMATE LOAD OF A-387 NOTCHED TENSION SPECIMEN

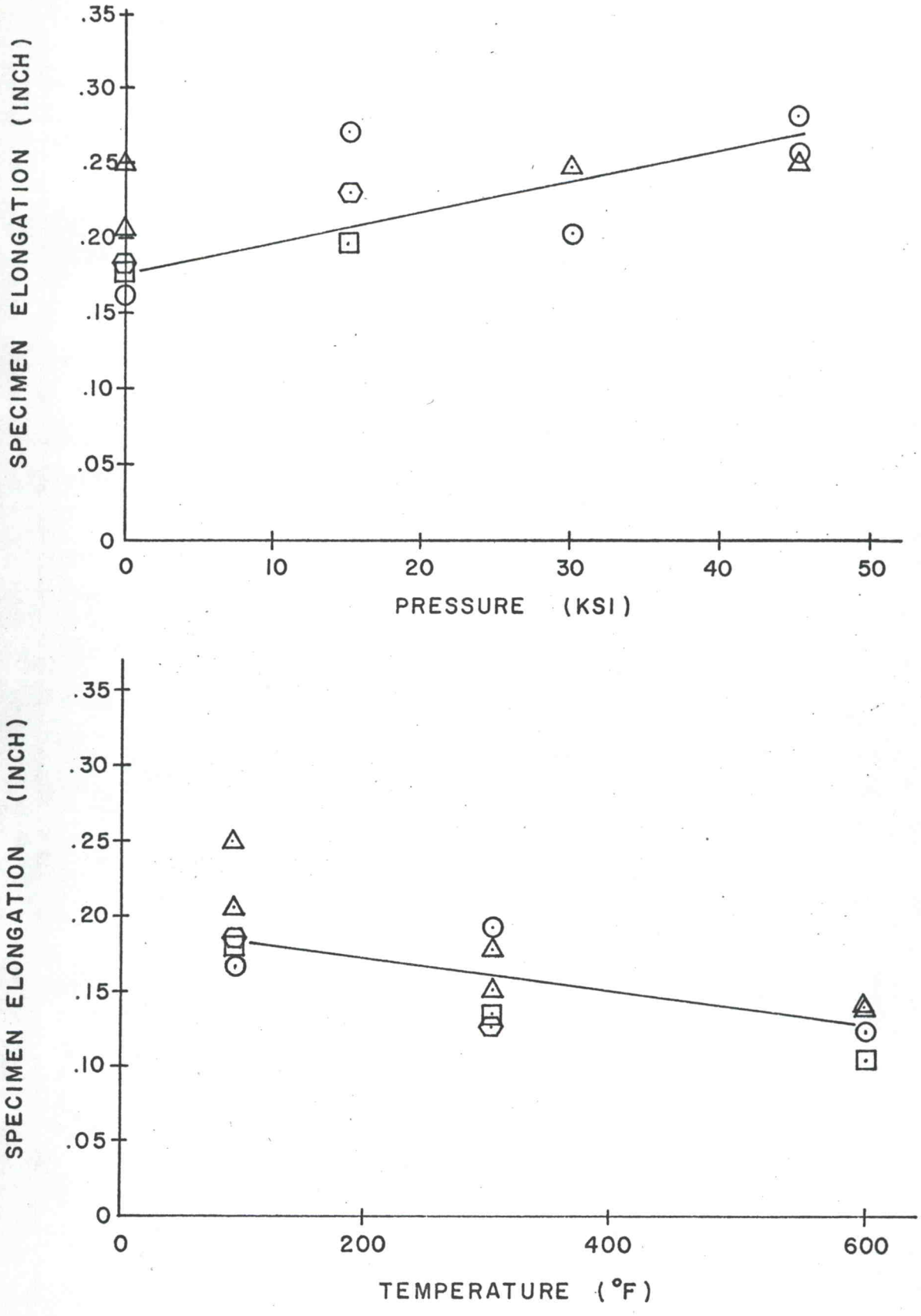


FIG. 16. EFFECTS OF ENVIRONMENTAL PRESSURE AND TEMPERATURE ON THE ELONGATION OF A-387 NOTCHED TENSION SPECIMEN

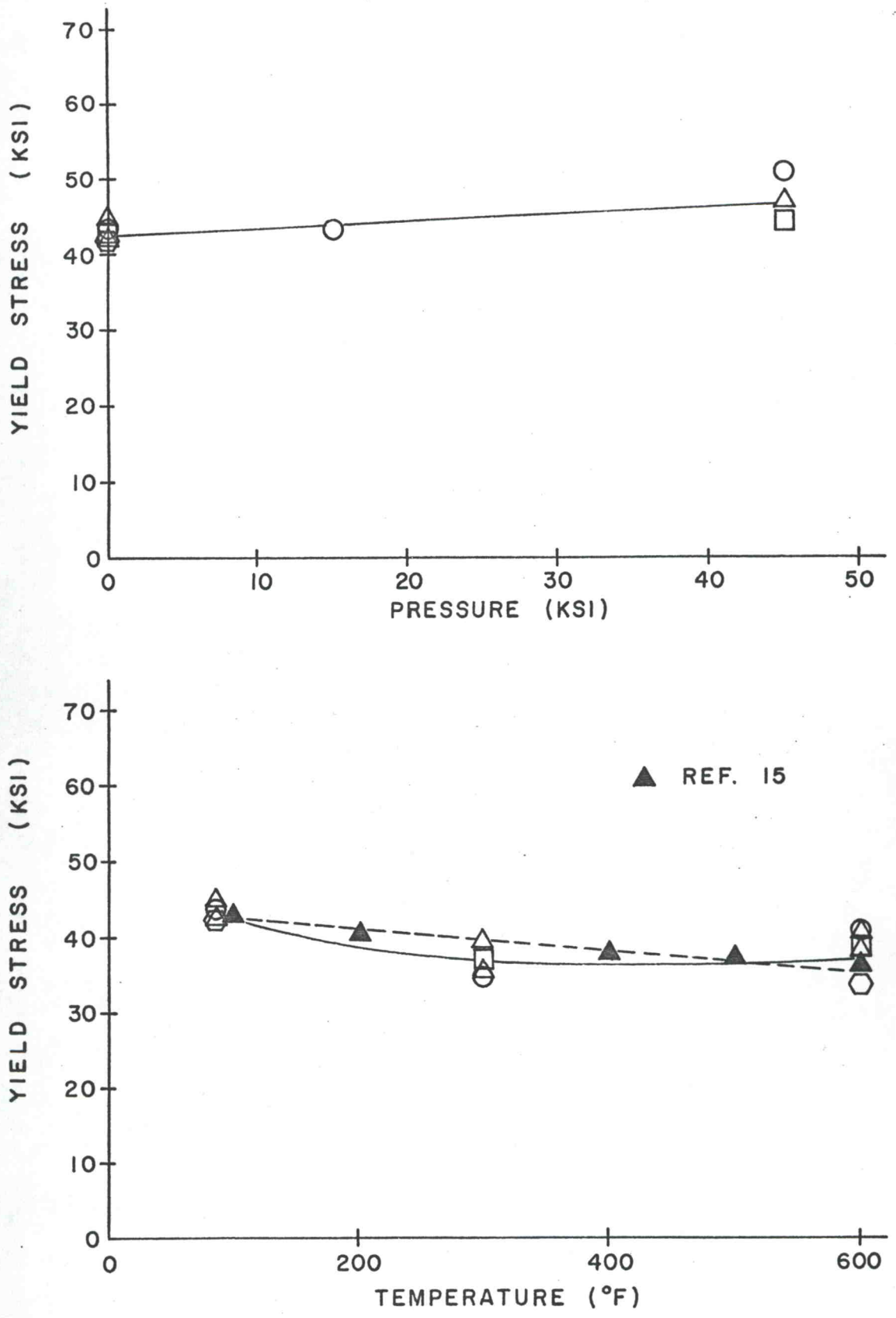
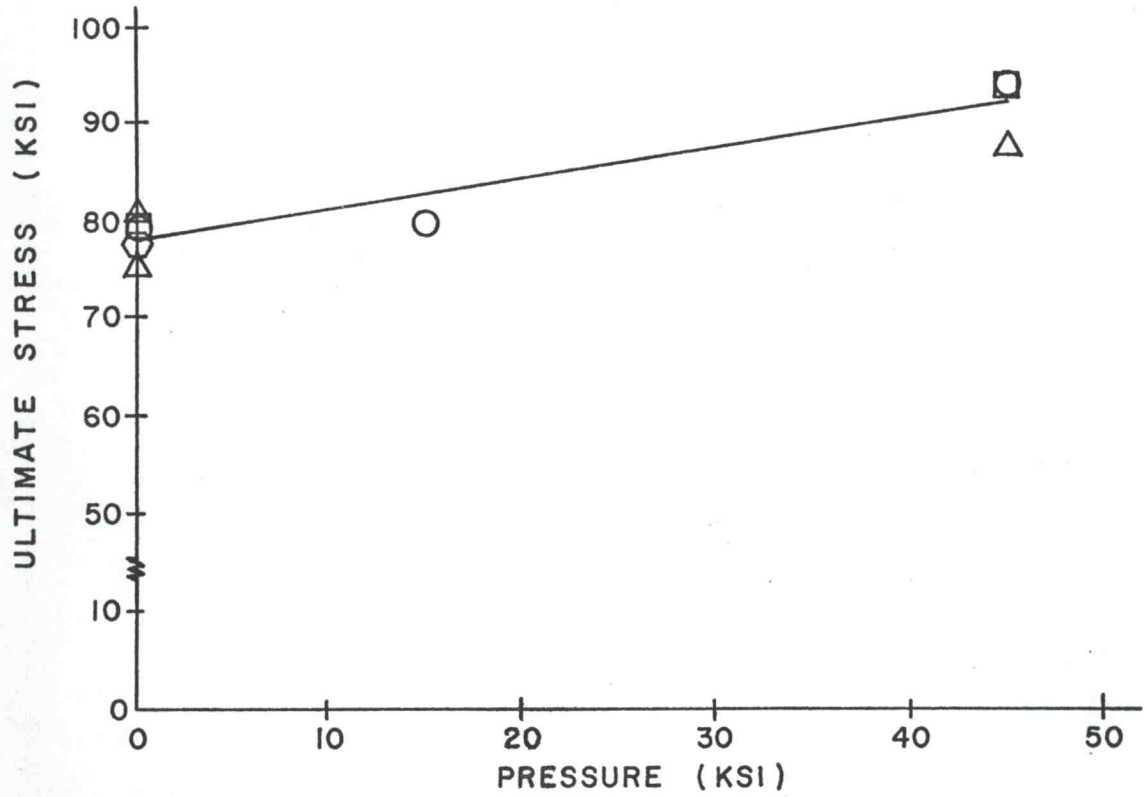


FIG. 17 EFFECTS OF ENVIRONMENTAL PRESSURE AND TEMPERATURE ON THE YIELD STRENGTH OF A-204 STEEL



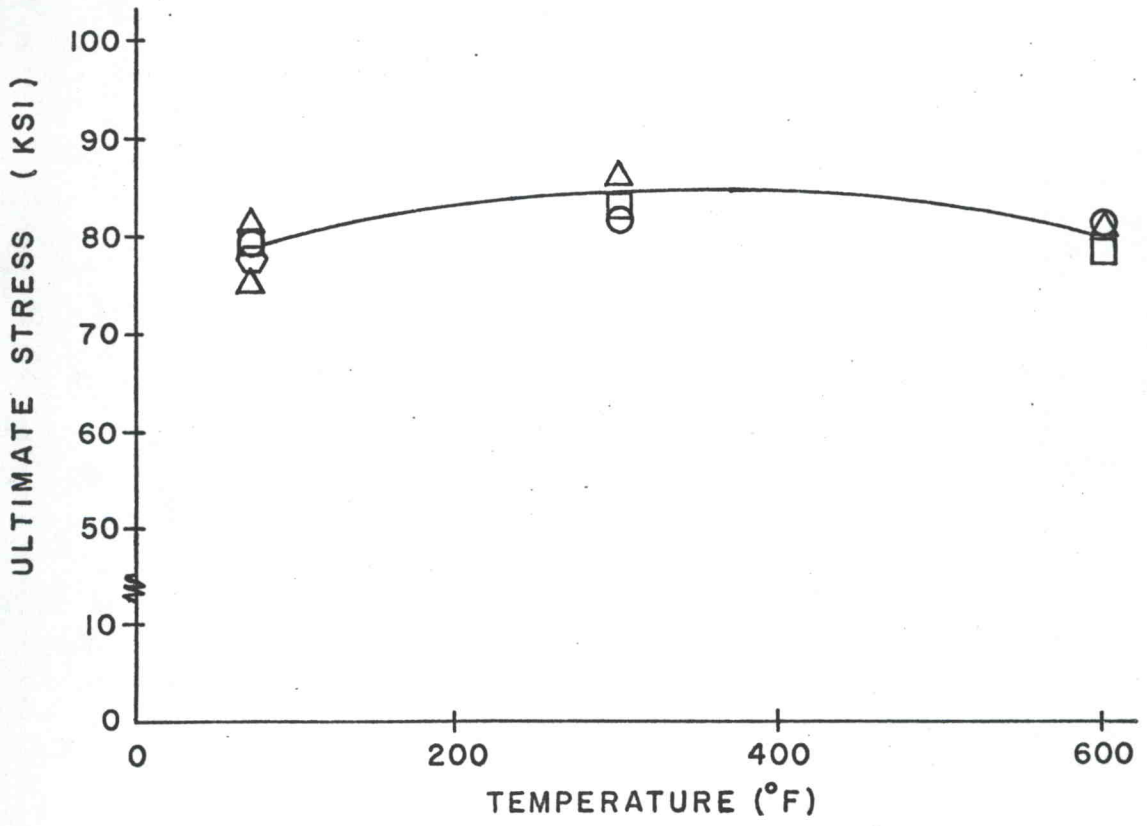
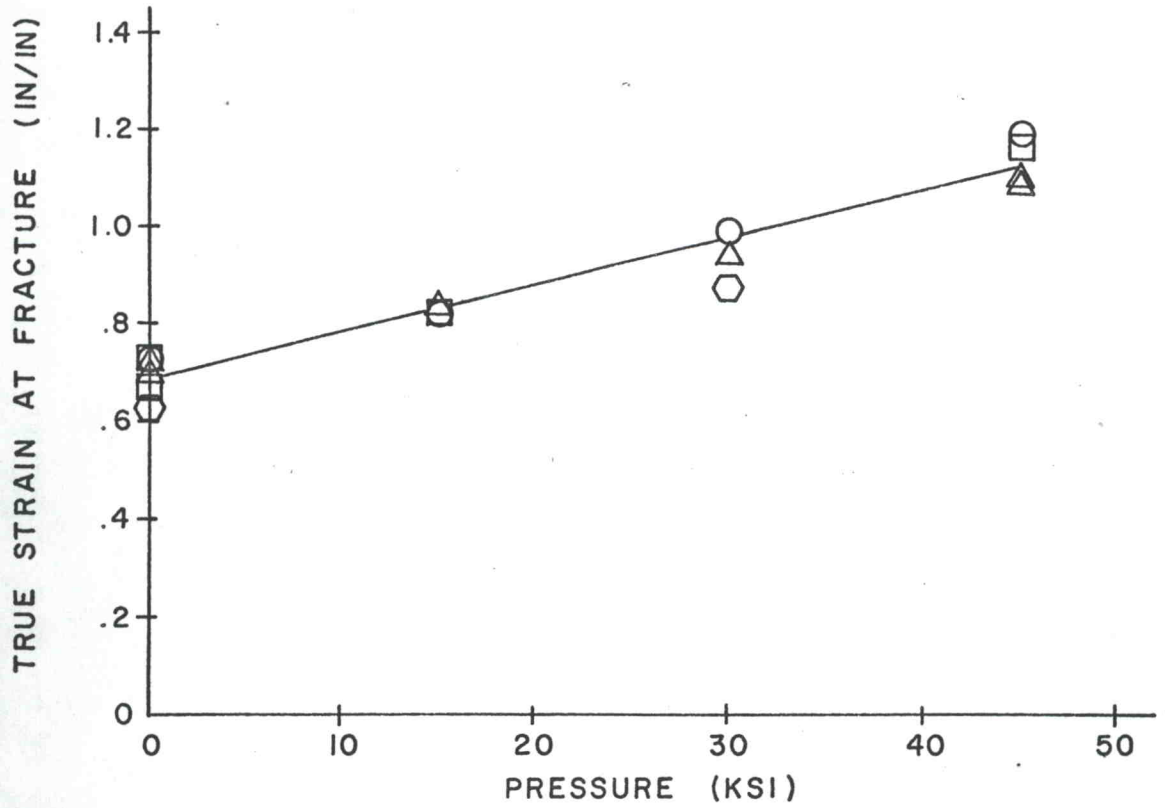


FIG. 18 EFFECTS OF ENVIRONMENTAL PRESSURE AND TEMPERATURE ON THE ULTIMATE STRENGTH OF A-204 STEEL



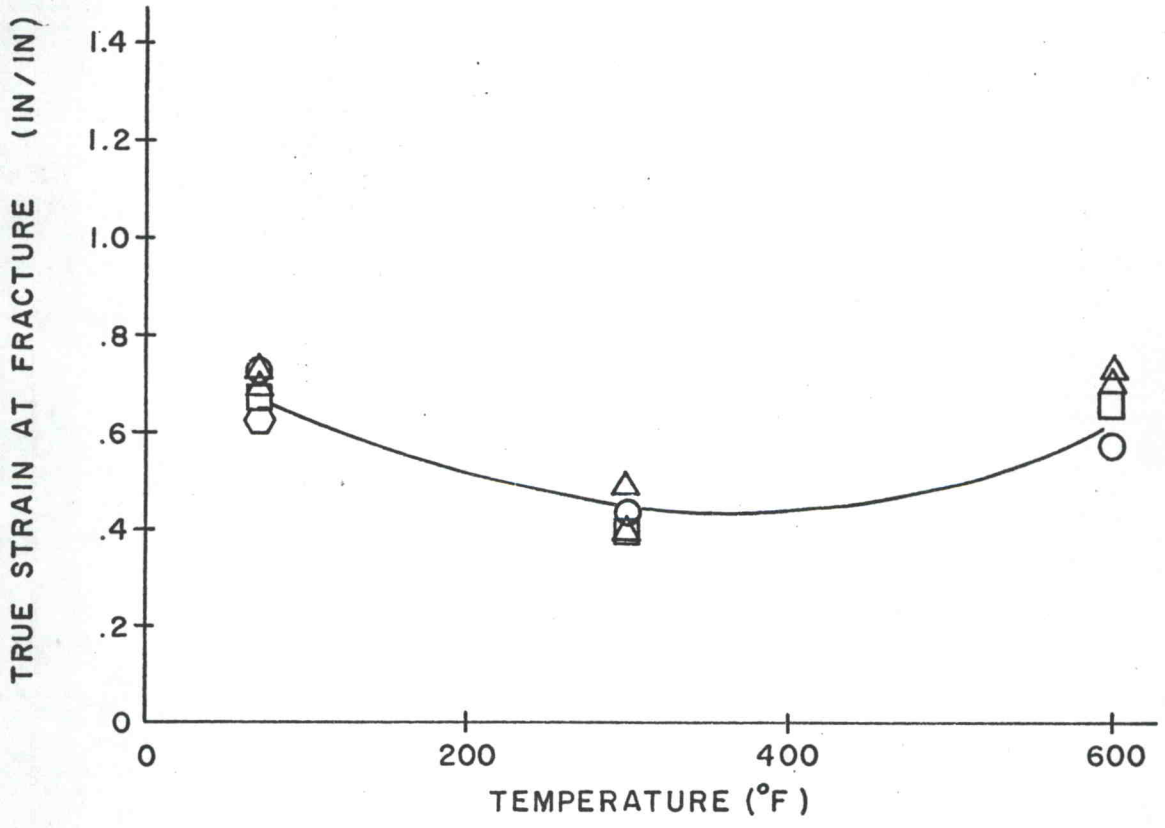
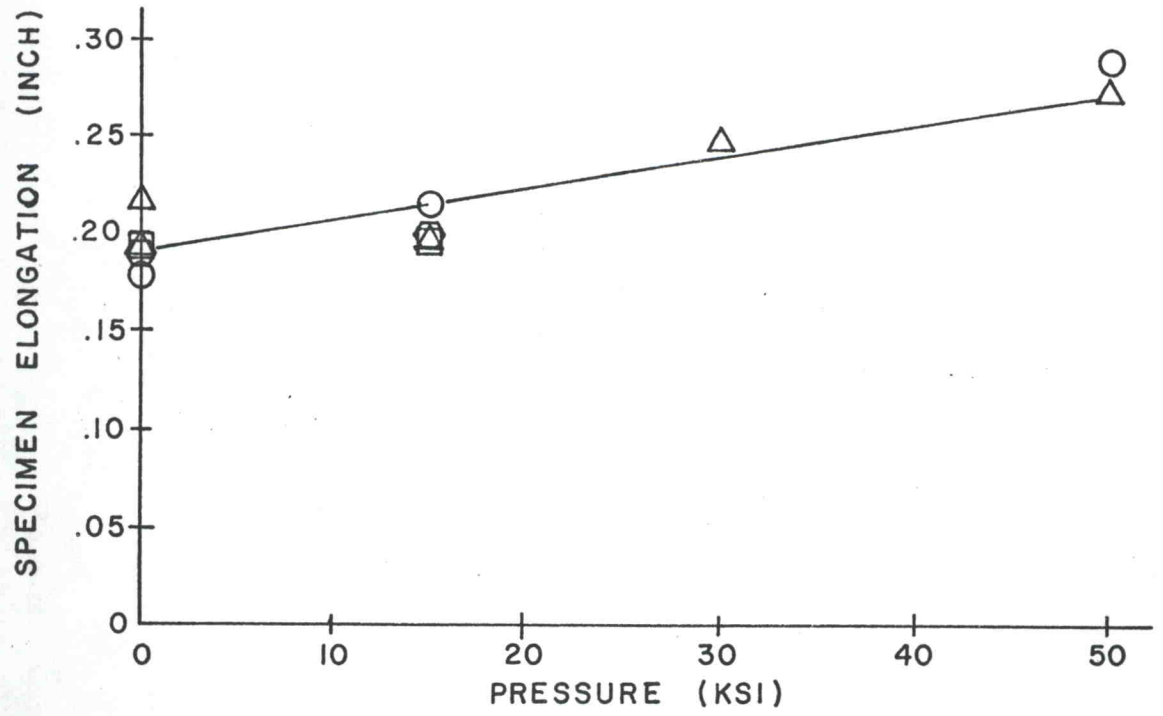


FIG. 19 EFFECTS OF ENVIRONMENTAL PRESSURE AND TEMPERATURE ON THE TRUE STRAIN AT FRACTURE OF A-204 STEEL



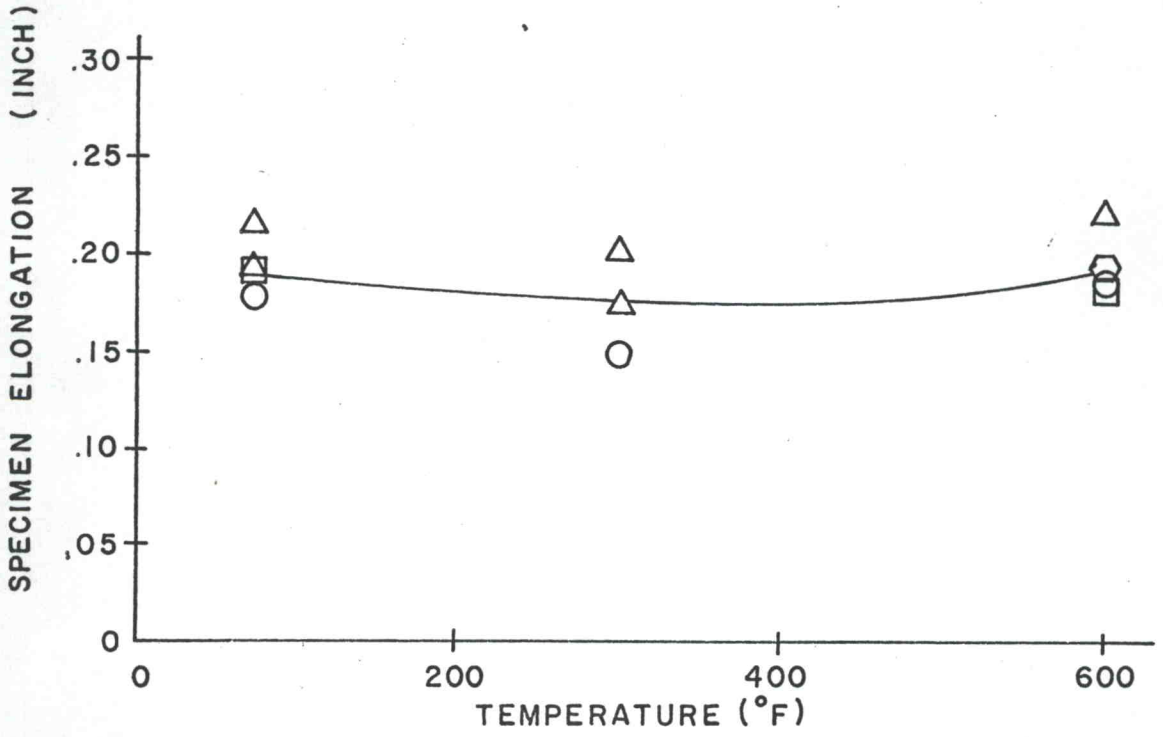


FIG. 20 EFFECTS OF ENVIRONMENTAL PRESSURE AND TEMPERATURE ON THE ELONGATION OF A-204 NOTCHED TENSION SPECIMEN

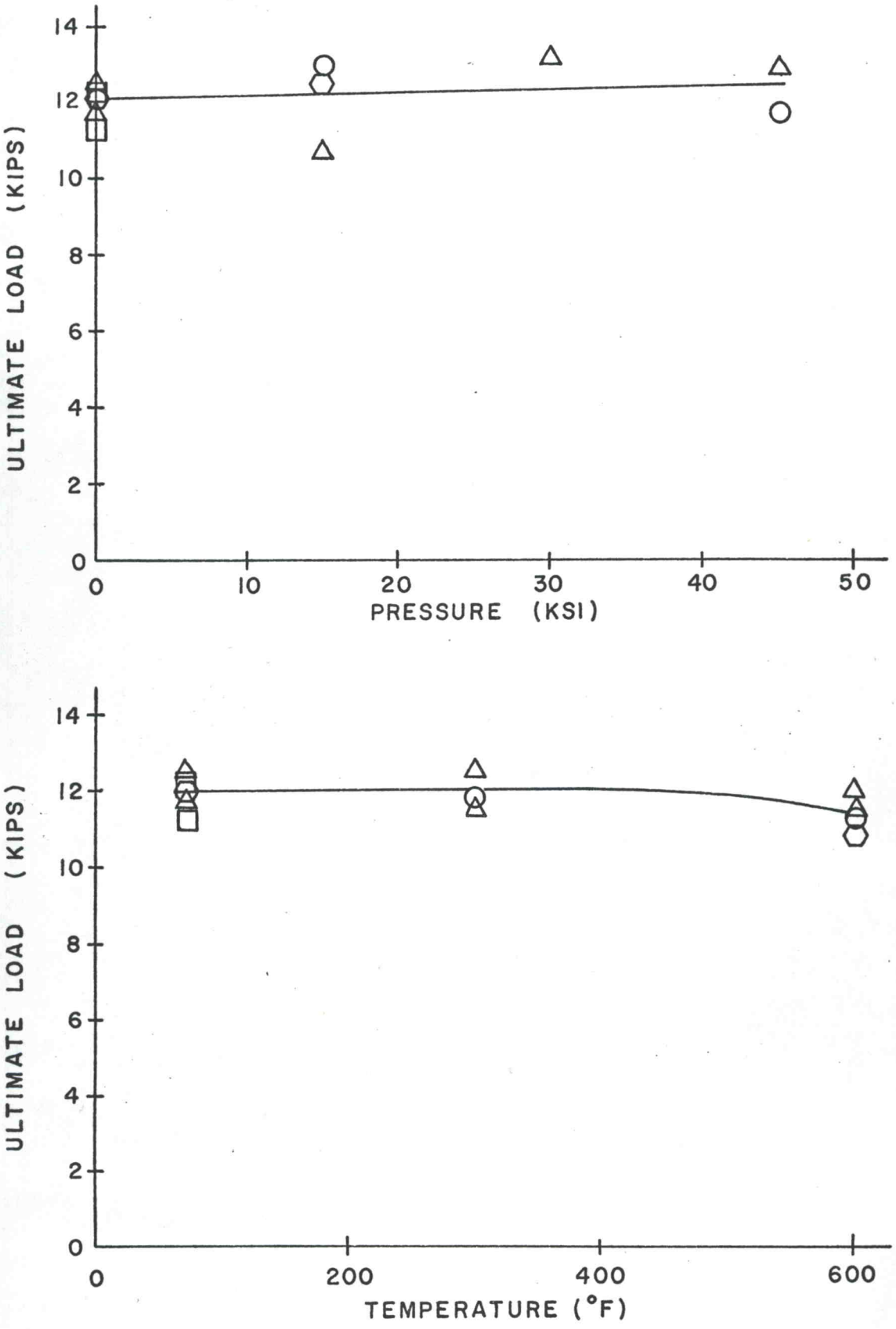


FIG. 21 EFFECTS OF ENVIRONMENTAL PRESSURE AND TEMPERATURE ON ULTIMATE LOAD OF A-204 NOTCHED TENSION SPECIMEN

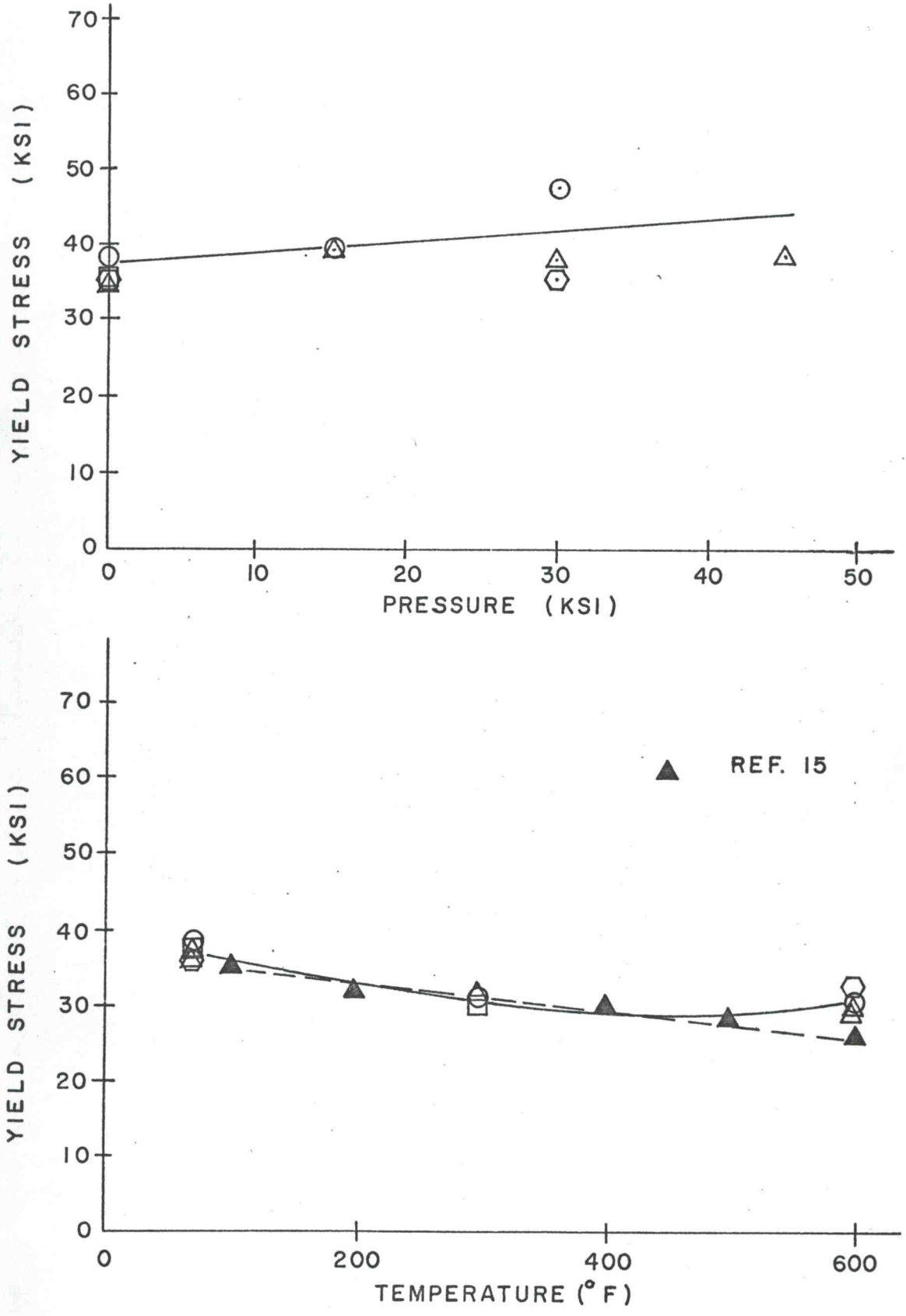


FIG. 22. EFFECTS OF ENVIRONMENTAL PRESSURE AND TEMPERATURE ON THE YIELD STRENGTH OF A-515 STEEL

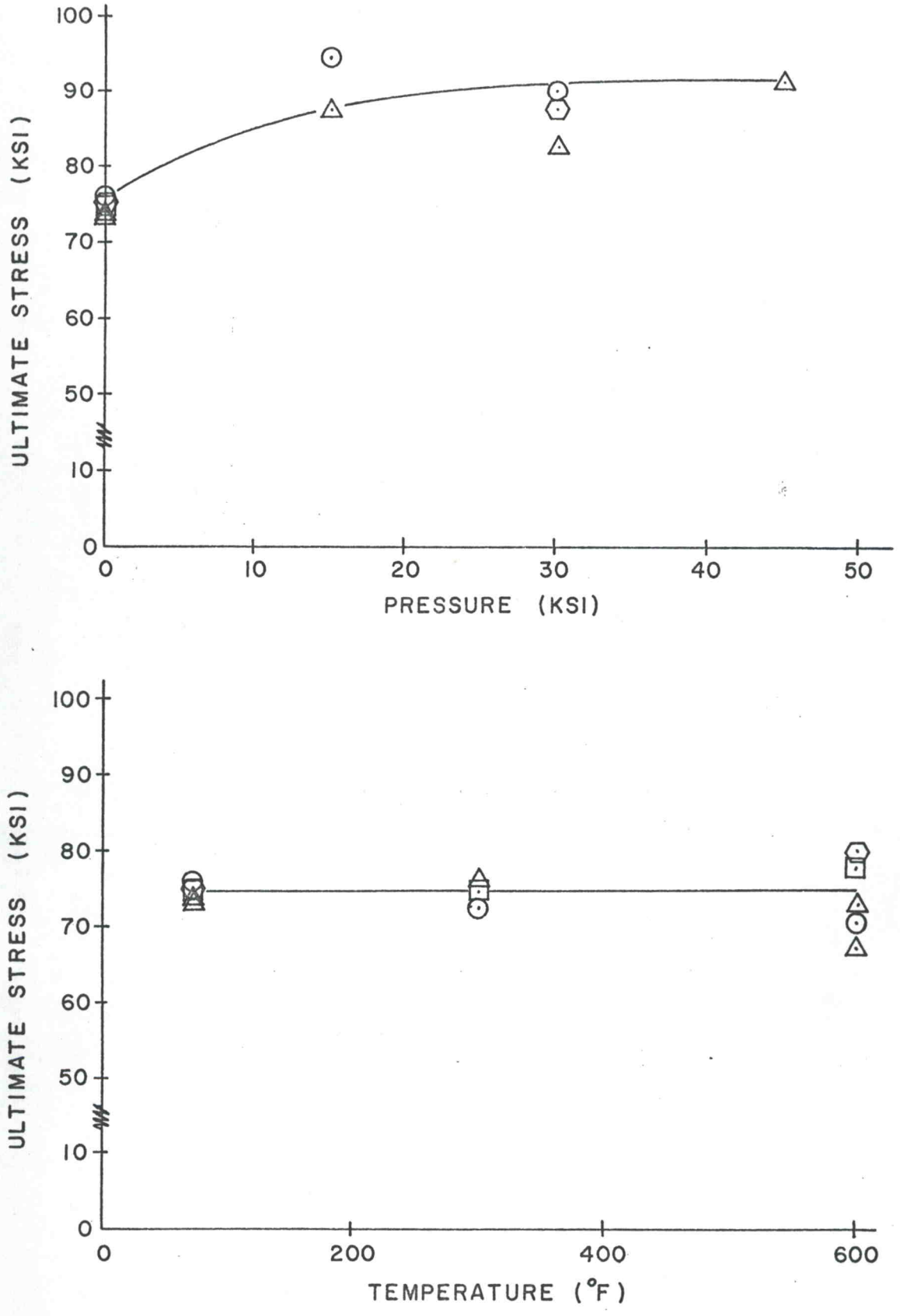
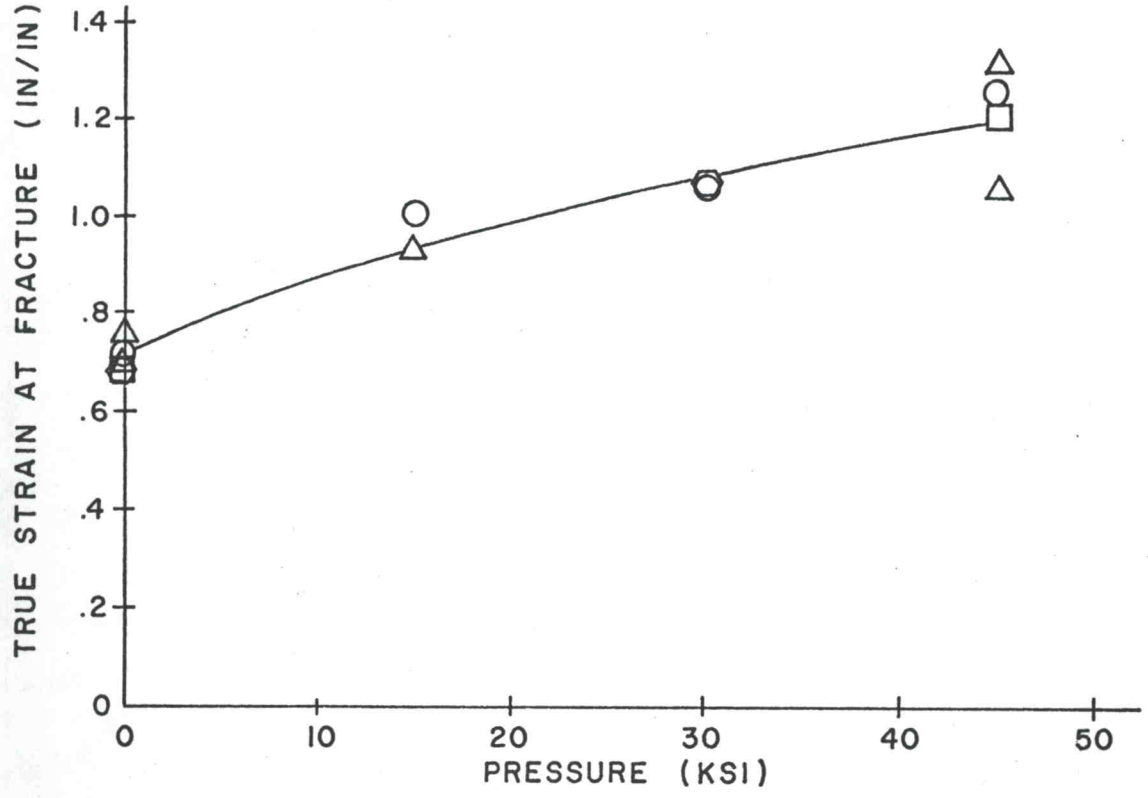


FIG. 23. EFFECTS OF ENVIRONMENTAL PRESSURE AND TEMPERATURE ON THE ULTIMATE STRENGTH OF A-515 STEEL



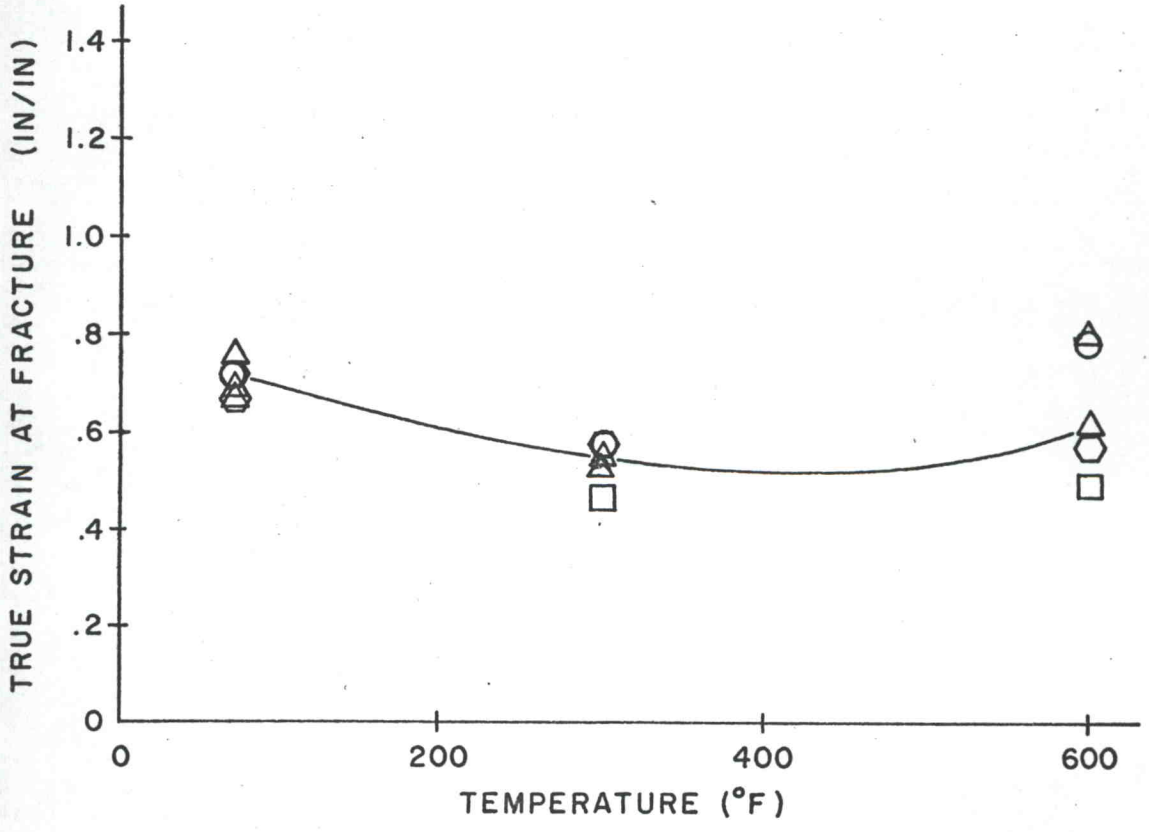


FIG. 24 EFFECTS OF ENVIRONMENTAL PRESSURE AND TEMPERATURE ON THE TRUE STRAIN AT FRACTURE OF A-515 STEEL

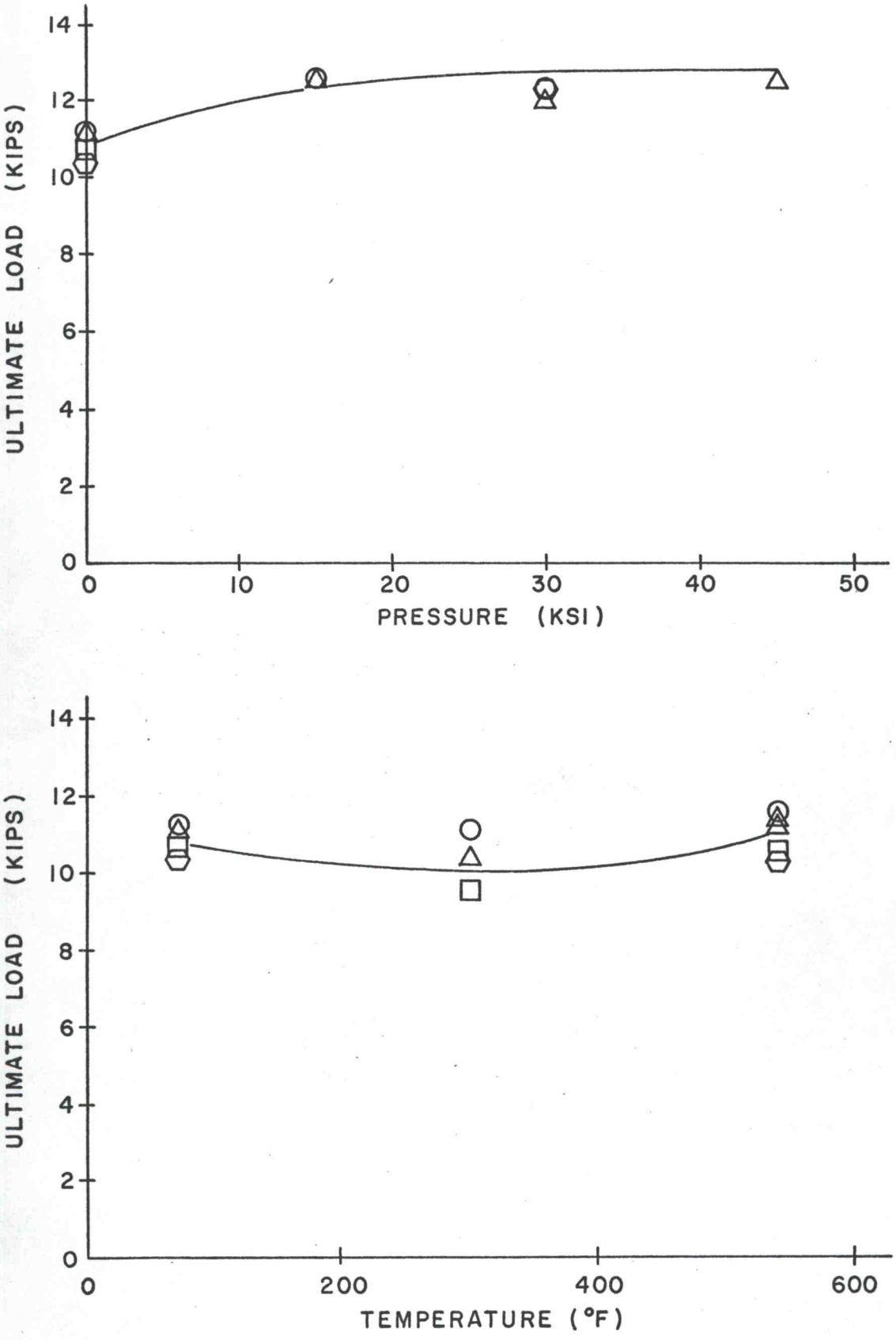
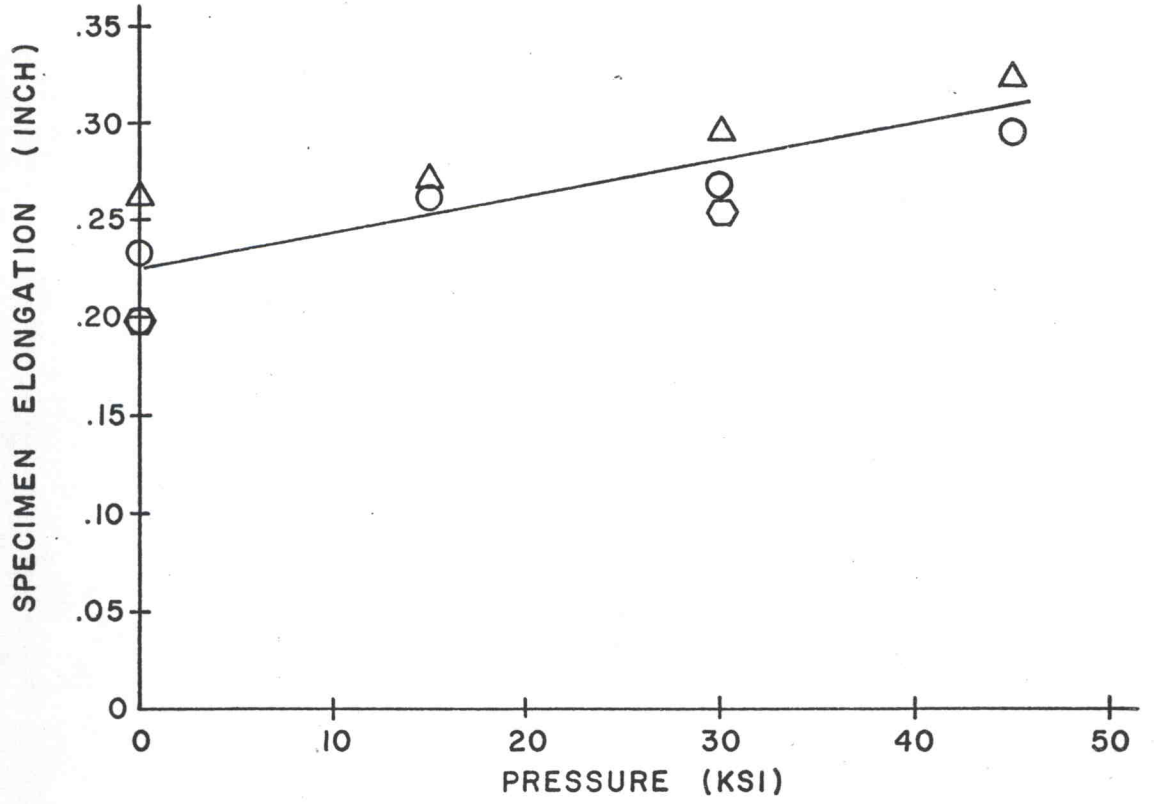


FIG. 25 EFFECTS OF ENVIRONMENTAL PRESSURE AND TEMPERATURE ON THE ULTIMATE LOAD OF A-515 NOTCHED TENSION SPECIMEN



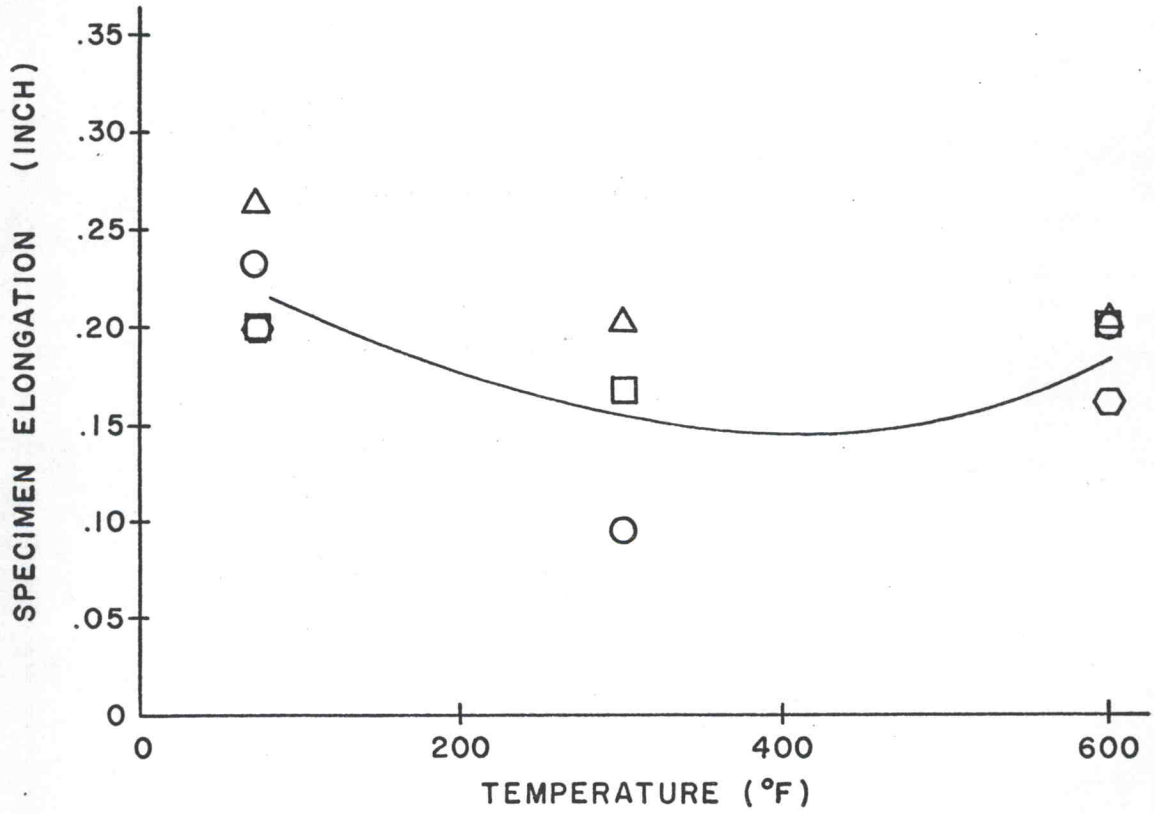


FIG. 26 EFFECTS OF ENVIRONMENTAL PRESSURE AND TEMPERATURE ON THE ELONGATION OF A-515 NOTCHED TENSION SPECIMEN

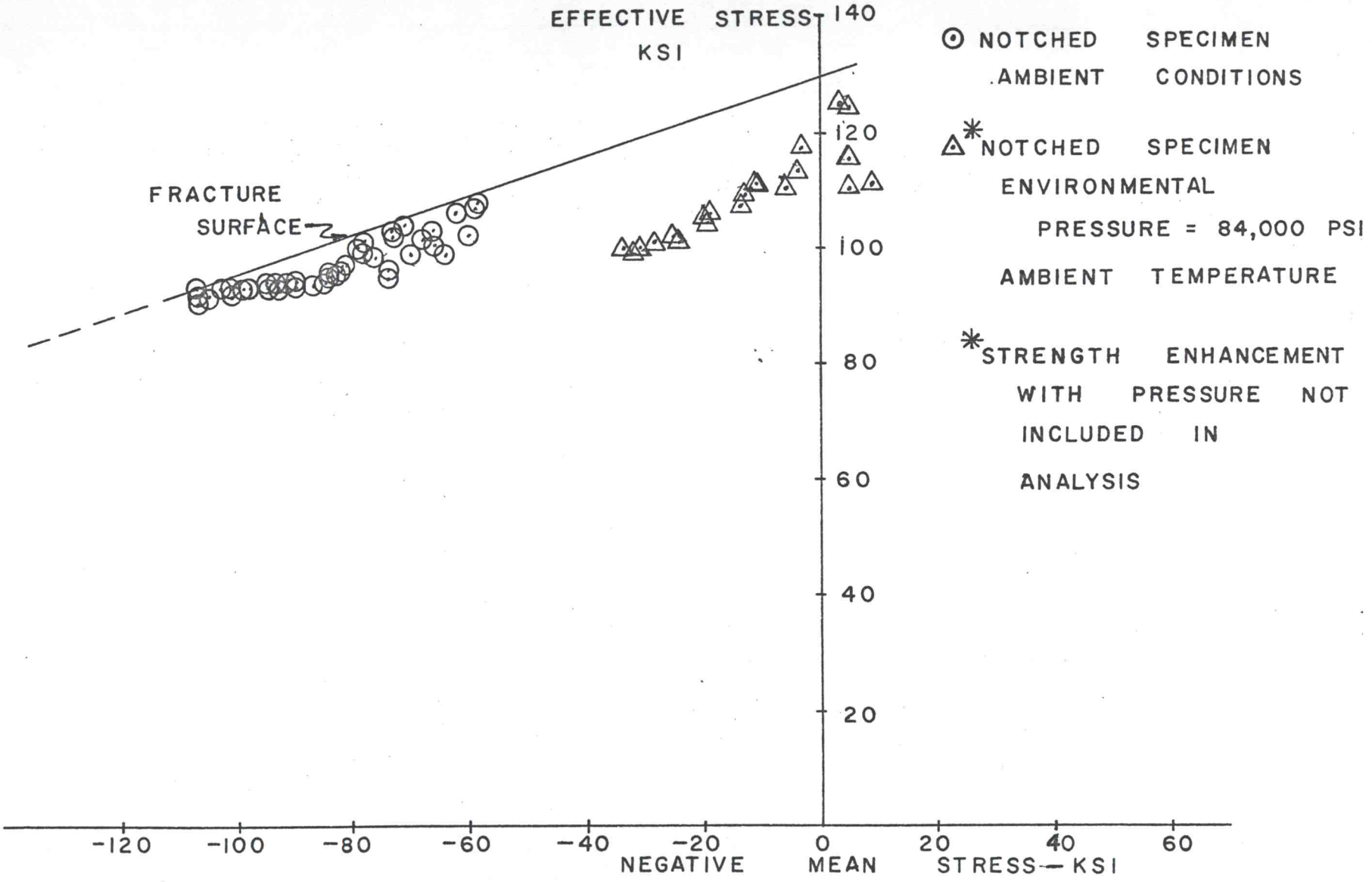


FIG. 27. CALCULATED EFFECTIVE STRESS — MEAN STRESS AT ULTIMATE LOAD FOR A-387 STEEL

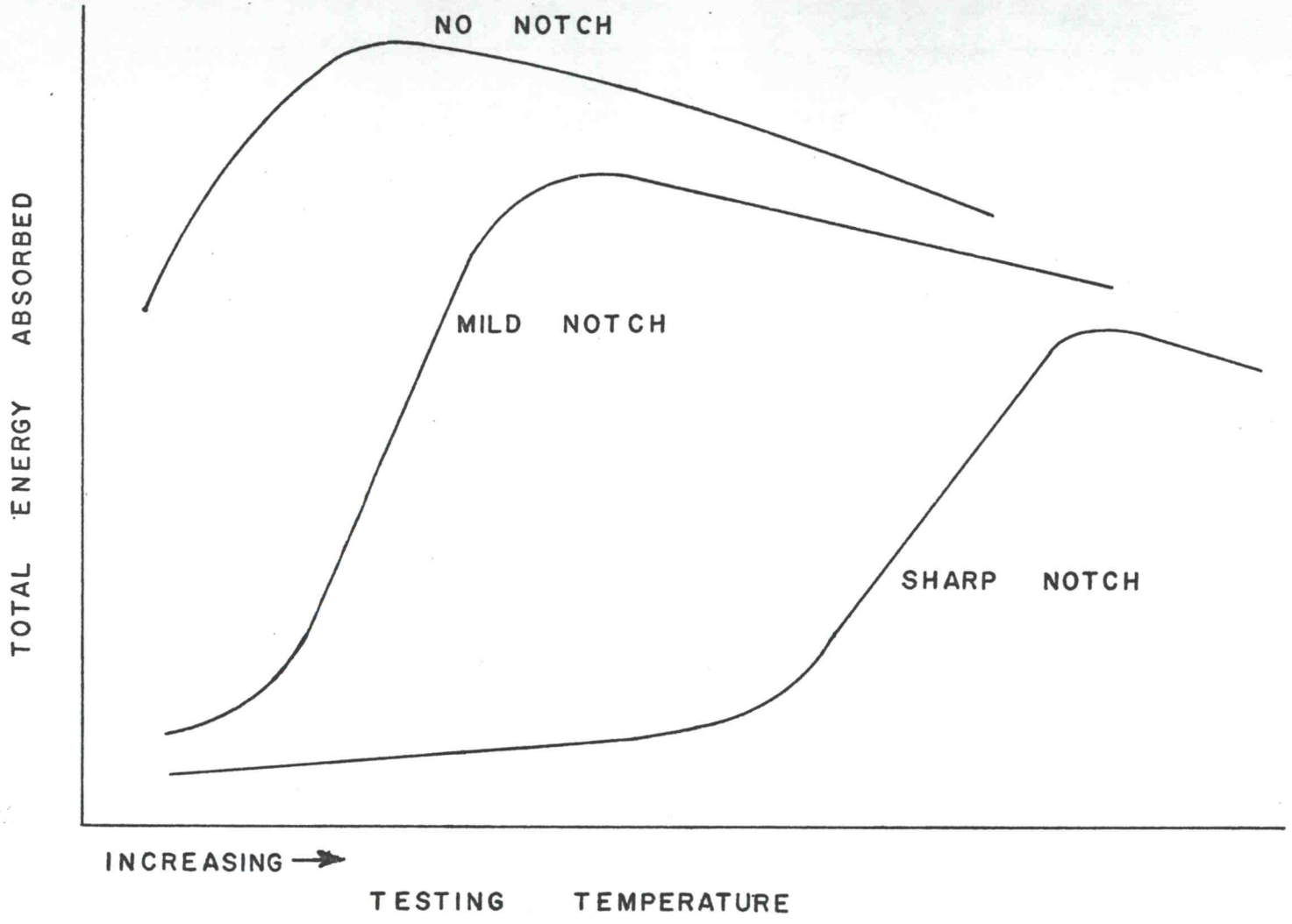


FIG. 28. EFFECTS OF NOTCH SEVERITY ON THE NIL DUCTILITY TRANSITION TEMPERATURE[6]

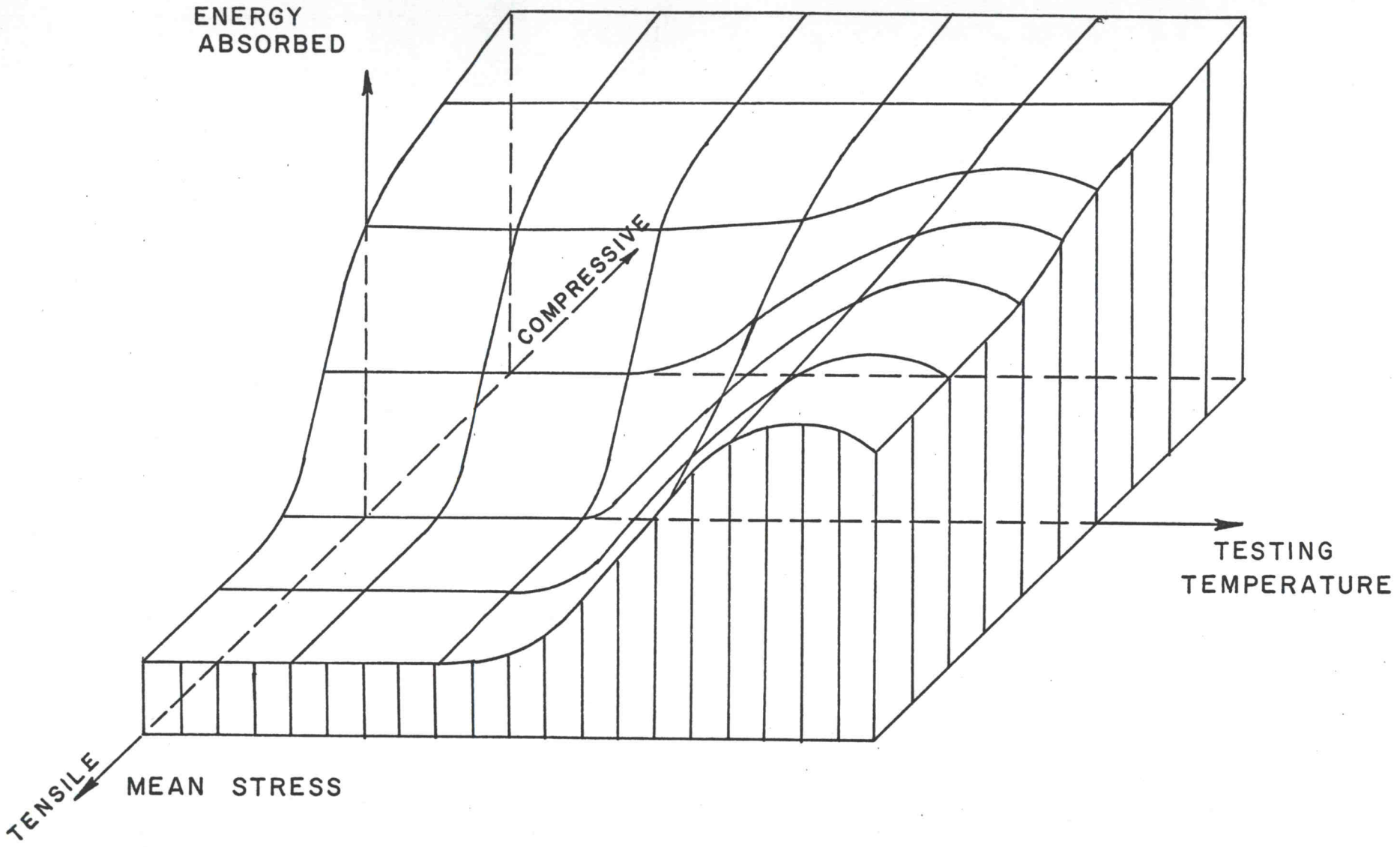


FIG. 29 EFFECTS OF STRESS STATE AND TEMPERATURE ON THE NIL DUCTILITY TRANSITION